

HYDROCARBON FLUID INCLUSION FLUORESCENCE: A REVIEW.

Nigel J.F. Blamey and Alan G. Ryder.*

Nanoscale Biophotonics Laboratory, School of Chemistry, National University of Ireland-Galway, Galway, H91 CF50, Ireland.

* Corresponding Author: Alan G. Ryder, Nanoscale Biophotonics Laboratory School of Chemistry, National University of Ireland – Galway, Galway, Ireland.

Tel: 353-(0)91-492943; **Fax:** 353-(0)91-750596;

Email: alan.ryder@nuigalway.ie

This is the corrected author version of the review article.

The full article, version of record is available at: https://doi.org/10.1007/978-0-387-88722-7_13 :]

Please Cite as:

Blamey N.J., Ryder A.G. (2009) Hydrocarbon Fluid Inclusion Fluorescence: *A Review*. In: *Reviews in Fluorescence 2007*. *Reviews in Fluorescence*, vol 2007. Springer, New York, NY. https://doi.org/10.1007/978-0-387-88722-7_13

ABSTRACT

Geological fluid inclusions are small voids that can contain a variety of liquids which are often found in natural minerals and rocks. Typically, they are less than 10 micrometres in size that host fossil fluids which existed when the minerals grew or healed after fracture. Of particular interest to the petroleum industry are inclusions that contain hydrocarbon fluids, which originated from petroleum that once migrated through the rocks before becoming trapped. These hydrocarbon-bearing fluid inclusions (HCFI) are useful for learning about the processes, fluid compositions, temperatures and pressure conditions in geologic systems such as the migration of hydrocarbon fluids in petroleum basins. The accurate characterisation of the petroleum fluid entrapped in inclusions presents the analyst with considerable challenges. HCFI samples are very valuable (usually obtained from core drilling) and thus a non-contact, non-destructive, analytical method is required. The small size of HCFI necessitates the use of microscopy-based techniques while spectroscopic methods are needed to characterise the chemical composition. Fluorescence based methods offer the best combination of high sensitivity, diagnostic potential, and relatively uncomplicated instrumentation. It is the fluorescence of HCFI and the spectroscopic methods employed for their analysis which is the focus of this review. Specific sections focus on the description of HCFI, petroleum fluorescence, and microscopic techniques. The review and discussion focuses primarily on advances and studies reported in the literature from 1980's onwards, and outlines some of the issues that need to be addressed to make fluorescence methods more reproducible and quantitative for HCFI analysis.

INTRODUCTION

In a geological context, fluid inclusions are small voids, which are found in natural minerals and rocks, that can contain a variety of liquids. They may be regarded as small sealed vials, often less than 10 micrometres in size, that host fossil fluids which existed when the minerals grew or healed after fracture (1). The composition of fluid inclusions varies considerably, and may comprise of liquid, solid, and/or gaseous phases, depending on the fluid source and the pressures-temperatures experienced. These phases commonly include water, dissolved gases, and salts; in extreme cases inclusions may host daughter minerals, high-pressure vapour phases, and complex organic mixtures. Of particular interest to the petroleum industry are those inclusions that contain hydrocarbon fluids, which originated from petroleum that once migrated through the rocks before becoming trapped within inclusions (2).

Fluid inclusions, despite their small size, are highly valuable to understanding many geological processes. When these cavities within the rock were sealed, they trapped the original fluid at these fossil pressure-volume-temperature (PVT) conditions. This PVT data can be used for modelling fluid phase behaviour and give an indication of the “oil window” at which oil formation occurs (2). Geologists can learn much about the processes, fluid compositions, temperatures and pressure conditions in geologic systems from fluid inclusions that form at a key time, such as during ore formation in base-metal or gold deposits, or from the migration of hydrocarbon fluids in petroleum basins. Not all fluid inclusions present within a sample may represent the key event that the geologist is studying and therefore an experienced fluid inclusion analyst is needed to examine the paragenetic relationships between fluid inclusion assemblages, mineral growth or fracture healing. By so doing, the geologist is able to study the migration of fluids, including petroleum fluids, and understand what processes led to the migration or trapping of petroleum.

Hydrocarbon-bearing fluid inclusions (HCFI) generally occur in diagenetic cements or grains and contain complex mixtures of mainly organic compounds depending on their source/s. Accurate analysis of the chemical composition of the entrapped hydrocarbons in HCFI can yield vital information about the history, evolution and migration of petroleum fluids, and is thus crucial data for the petroleum exploration industry. Studying HCFI is advantageous because the trapped fluids are representative of the actual hydrocarbon fluids that existed when the inclusions were sealed in the mineral. This sealing in process, preserves the petroleum fluid, thus isolating it from subsequent infiltration of petroleum fluids and events in oil reservoirs such as loss of charge, water washing, or biodegradation. It also preserves the fluid from contamination during the drilling processes used to extract samples from the ground (3).

The accurate characterisation of the fluid entrapped in inclusions presents the analyst with considerable challenges. HCFI samples are very valuable (usually obtained from core drilling) and thus a non-contact, non-destructive, analytical method is required. The small size of HCFI necessitates the use of microscopy based techniques and fluorescence spectroscopy offers the best combination of high sensitivity, diagnostic potential, and relatively uncomplicated instrumentation. It is the fluorescence of HCFI and the spectroscopic methods employed for analysis which is the focus of this review. Specific sections focus on the description of HCFI, petroleum fluorescence, and microscopic techniques. The review and discussion focuses primarily on advances and studies reported in

the literature from 1980's onwards, and outlines some of the issues that need to be addressed to make fluorescence methods more reproducible and quantitative for HCFI analysis.

INCLUSIONS: *A brief description.*

Fluid inclusions are found in many different types of natural minerals and rocks. They may be regarded as small sealed vials, often less than 10 micrometres in size, that host fossil fluids which existed when minerals grew or healed after fracture (1). Fluid inclusion shapes vary widely from highly irregular to “negative crystals” where the host mineral crystal habit is mimicked by the inclusion. Fluid inclusion composition varies considerably, depending on the fluid source and temperatures, and may be host to aqueous or hydrocarbon liquids, solids, and gaseous phases. Aqueous fluid inclusions comprise mainly water with dissolved salts or daughter minerals along with minor dissolved inorganic, organic and trace noble gases whereas hydrocarbon-bearing fluid inclusions (HCFI) generally comprise liquid hydrocarbons, low carbon-number gases, and occasionally dark solid phases (see Figure 1).

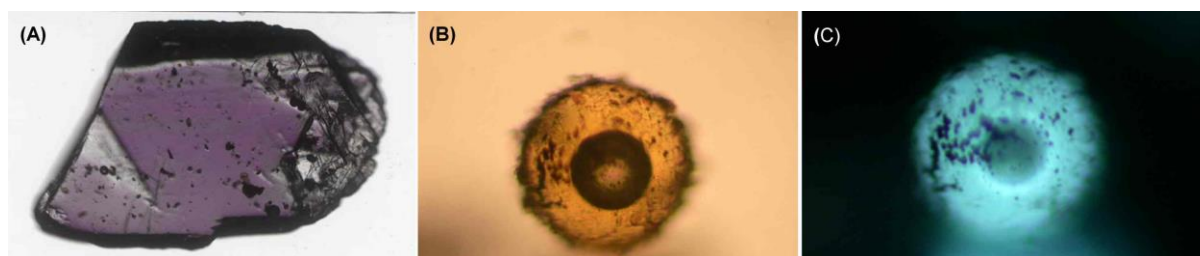


Figure 1: Images of a rock wafer containing inclusions (A), white light image of a liquid-vapour HCFI (B), and an epifluorescence image of the same inclusion using 366 nm excitation (C).

HCFI may occur both in reservoirs and in migration pathways, the most commonly documented are associated with reservoirs, and are trapped in diagenetic cements, overgrowths, or secondary fractures in quartz and feldspar. HCFI may develop at any time from the onset of reservoir filling to the present day, with trapping most likely during reservoir filling rather than later stages when the water is displaced (4). This may be attributed to quartz cementation being a slow, temperature mediated, process (5, 6) and that the micron-sized oil droplets sticking to the quartz grains inhibit quartz growth. The trapping of oil within a quartz cement may take millions of years whereas healing of secondary fractures is much more rapid, and may preserve the later stages of reservoir filling (3). The abundance of HCFI in clastic sediments may be correlated with porosity and permeability (7) whereas in chalk or limestone reservoirs the HCFI may be more irregular favouring cemented fractures, recrystallised fossils, or coarse-grained cement (2, 8, 9).

HCFI are not limited to petroleum reservoirs and they may also be found in a diversity of geological environments. For example, there is increasing evidence for the presence of HCFI within metal deposits (10, 11). Whether the presence of abundant organic compounds is an integral part of the mineralisation process may depend on specific ore deposit styles. For example, Mississippi-Valley-type (MVT) deposits commonly host HCFI, although their presence may be attributed to deep basinal brines that were primarily the

source of Pb- and Zn-bearing fluids.* Very old, Archaean rocks are also known to host HCFI, and they have been reported from the gold-bearing Witwatersrand Basin in South Africa (12, 13) and from the Pilbara Craton in Australia (14). The origins of hydrocarbons in these Archaean rocks is thought to be abiogenic (14). Other unusual geologic settings include impact craters (15, 16) and hydrothermal vents (17).

THE INCLUSION FLUIDS

The hydrocarbon fluid in HCFI may have highly complex compositions but are principally liquid with variable amounts of gas (light alkanes, CO₂, N₂, H₂S), paraffins, naphthalenes, aromatics, resins and sometimes waxes (2, 3, 9, 18). The apparent HCFI colour depends on a combination of the wavelengths absorbed by the various chromophores present in the trapped hydrocarbon liquid and the associated mineral environment. Consequently, their colour, when viewed under a microscope with plain white light illumination may vary considerably from transparent, to yellow, or dark brown, or black. The mineralogical properties which can also influence the perceived colour include birefringence, polarisation, reflectivity, and variations in refractive index.

One of the key methodologies in fluid inclusion study is micro-thermometry (1, 19). The sample containing the fluid inclusion(s) is placed in a chamber that can be either heated or cooled and then observed using a microscope while the temperature is varied. The temperatures at which phase changes occur are recorded thus providing information about homogenisation temperature, or brine salinity (for aqueous inclusions), or other data. HCFI provide fewer phase changes but they do fluoresce under UV or visible light illumination which can provide another source of information about fluid composition. The petroleum composition of HCFI is typically obtained by crushing a small amount of the HCFI containing material and extracting the petroleum fluid for analysis by gas chromatography (20) and mass spectrometry (21). The key disadvantages of the crush method are the destruction of the sample, probable mixing of fluids from different source inclusions, and potential contamination. Therefore, the oil composition data derived from these bulk analyses have to be carefully considered as the mixing of heterogeneous fluid inclusion populations may have occurred. The non-destructive quantitative analysis of individual HCFIs is therefore a desirable goal for those studying petroleum migration and is best achieved via optical methods. Optical methods have several general advantages that include: non-destructive/ non-contact analysis, reasonable sensitivity, ability to undertake micron-scale analysis of single inclusions, mature technology and methodologies, high diagnostic potential, and relatively simple instrumentation (22, 23).

FLUORESCENCE OF CRUDE OILS

The fluorescence of crude petroleum oils has been reviewed in detail previously (24). Briefly, the fluorescence emission is due to the presence of a multitude of aromatic hydrocarbons in varying concentrations. The nature of the emission is governed by the complex interplay between reabsorption, energy transfer, and quenching caused by the high concentrations of fluorophores and quenchers in petroleum oils. The complexity of crude oils usually prevents the resolution of any specific chemical component in terms of fluorescence

* Basinal brines are responsible for transporting hydrocarbons from deep basins where the hydrocarbons were generated from plant or animal matter.

emission parameters. Factors such as the specific chemical composition (concentration of fluorophores and quenching species) and physical (viscosity and optical density) control emission properties such as emission and excitation intensity, emission and excitation wavelength, and fluorescence lifetime. Generally, light oils (high API gravity) have relatively narrow, intense fluorescence emission bands with small Stokes' shifts. In contrast heavy oils (low API gravity) have emissions that tend to be broader, weaker, and red-shifted. The differences in emissions are attributed to a higher concentration of fluorophores and quenchers present in the heavier oils, thus leading to an increased rate of energy transfer and quenching to produce broader, weaker, red-shifted emissions (25, 26).

Since crude petroleum oils have very complex compositions, the excitation wavelength is of fundamental importance because changing wavelengths will result in the excitation of different fluorophore populations, which in turn can result in dramatic changes in the emission properties. Longer excitation wavelengths result in a narrowing of the fluorescence emission bands, along with a reduction in Stokes' shifts, fluorescence lifetime, and quantum yields (24–28). This is attributed to excitation of different fluorophores which changes the rates of fluorescence emission, quenching, and energy transfer (26, 28, 29). There have been many fluorescence studies of crude petroleum oils and several sources have correlated steady-state emission properties to oil composition. Using a 365 ± 30 nm excitation source, the wavelength of maximum fluorescence emission (λ_{max}) was shown to correlate with API gravity (30) and the aromatic composition (31) of crude oils. A ratio of fluorescence intensity at 650 and 500 nm (known as $Q_{R/G}$ or red-green quotient) was seen to correlate with viscosity (30), API gravity and composition from selected Canadian crude oils (31, 32). A similar parameter ($Q-535$) based on the ratio between the 535-750 nm flux and 430-535 nm flux using 365 nm excitation was also used to characterise crude oils and HCFI but no quantitative correlation to petroleum composition was described (22, 33). The $Q-535$ value decreases with increasing oil maturity, i.e. bluer fluorescing inclusions.†

One bulk optical method used for analysis of trace fluorescence on grain surfaces as well as oil inclusions is the Quantitative Grain Fluorescence (QGF) and Quantitative Grain Fluorescence on Extract (QGF-E) methods developed by CSIRO (34). This is a bulk fluorescence method that uses a slightly modified standard fluorescence spectrometer, where a narrow band interference filter is added in the excitation pathlength to provide a precise excitation wavelength in the UV (254 nm for QGF and 260 nm for QGF-E). The continuous emission spectrum from 300-600 nm is generally measured and this data used to calculate a QGF index, which is defined as the average spectral intensity between 375 nm (I_{375}) and 475 nm (I_{475}) normalised to the spectral intensity at 300 nm. The authors also, rather confusingly define a QGF ratio which is the ratio between the average spectral intensity of 375–475 nm and the spectral intensity at 350 nm. The spectrum of condensate and light oils are generally skewed towards the shorter wavelengths (~400 and ~450 nm peak maxima respectively) whereas the heavier oils have broader and more red-shifted emission maxima (~475 nm for an oil with an API gravity of 25). Isolated tetra-aromatic and polar fractions (from liquid chromatography) have spectral maxima which are even further red shifted to ~475-500 and 550 nm respectively. Dilution of the isolated fractions in hexane results in blue shifted emission spectra particularly for the tetra-aromatics. The QGF index has been used to infer

† Hydrocarbon gas content generally indicates the maturity of an oil, controlled by the degree to which it has been heated to induce breakdown of large organic molecules to form oil and gas. Immature oils have low gas content (methane is dominant), whereas mature oils have moderate gas content with high ethane and propane concentrations; finally overmature oils have high methane contents.

relative palaeo-oil saturation (34) and discriminate different oil types according to maturity (35).

HCFI FLUORESCENCE

HCFI may easily be mistaken for aqueous-bearing fluid inclusions during a first-pass inspection using optical petrography in transmitted light mode because many HCFI are colourless or slightly brown with a vapour bubble and thus resemble aqueous-dominated fluid inclusions. Excitation by UV illumination is the routine preliminary method for identifying HCFI in thin section thus discriminating them from aqueous inclusions. Aqueous fluid inclusions (AFI) generally do not fluoresce although weak scattering of UV light may, in rare cases, mislead the observer into mistaking AFI for a weak violet fluorescing HCFI. The petroleum fluids within HCFI fluoresce when illuminated by light of a sufficiently energetic wavelength, in practice this can be achieved with light from the UV to the NIR region of the spectrum (24). The earliest paper to describe HCFI fluorescence may be one by Murray in 1957 (36), but it was the increased availability of fluorescence microscopes during the 1980's that empowered those studying HCFI to commence active research using fluorescence methods (37, 38). Since then there has been an extensive literature on the subject, and the analysis of HCFI by fluorescence methods is now very common (2, 39).

However, despite the fact that the fluorescent properties of crude petroleum oils have been widely studied (24) the linking of fluid inclusion composition to crude oil composition is not always straightforward (2, 20, 40). The most important caveat is that most bulk oil studies involve the use of “*dead*” oils where there has been a loss (intentional or otherwise) in the light alkane and gaseous fractions from the oils prior to analysis. A loss in light fraction alkanes tends to result in additional fluorescence quenching, which manifests itself as weaker emission and shorter lifetimes. When one considers HCFI, many of the inclusions, because they are sealed, should retain a significant light gaseous fraction and therefore the oil is termed “*live*”. These live oils tend to have stronger, bluer, and longer lived fluorescence lifetimes because of the dilution effect from the gaseous alkanes. This creates a difficulty in creating calibration correlations with bulk crude oils that have been topped prior to compositional analysis.‡ Therefore, assuming that fluorescence responses of “*dead*” oils are exactly the same as “*live*” HCFI can lead to incorrect conclusions. Another consideration for HCFI studies is that the reference oils should be sourced from the same locality (31, 41), to avoid the wide fluorescence variances found between oils from different sources which have similar API gravity (24).

Recently the use of diamond anvil cells (42) coupled with fluorescence detection has allowed crude petroleum oils to be subjected to typical geological burial temperatures and pressures, and the changes in emission properties monitored. The method has also been used to explore the formation of petroleum oils from different sources (43, 44). In the 2008 study (44) the authors clearly demonstrate the progressive blue shift (λ_{\max}) and increase in emission intensity as the kerogen based materials undergo thermal maturation, and petroleum oil is formed. The data presented suggest that the λ_{\max} of spectra for inclusion oils will shift in a similar direction despite differences in composition or source kerogen. It is hoped that these studies will be extended to the collection of fluorescence lifetime data which could give a

‡ Topped oils are those in which the light fraction is intentionally removed by heating to 60°C (typically) prior to analysis.

more complete insight to both oil formation and maturation processes. The method looks very promising for the development of reproducible oil maturity calibration models that then can be applied to HCFI analysis.

Another approach to the development of standards for HCFI fluorescence analysis has been the use of synthetic fluid inclusions. Synthetic hydrocarbon-bearing fluid inclusions can be generated using a variety of materials including KCl (23), NaCl (31), phosphates (45), and quartz (46). For soluble salts the general procedure is to add some petroleum oil to a supersaturated solution of the salt followed by a slow evaporation to form crystals (31). Unfortunately, the process of evaporation, crystal growth, and inclusion formation is not conducive to the homogeneous trapping of the petroleum fluids. The fluid can be partitioned into different fractions according to changes in affinity for crystal surfaces and the aqueous layer. An additional factor to consider is the fact that the petroleum fluid entrapped in synthetic fluid inclusions will be a “dead” oil, lacking the lighter gaseous hydrocarbons.

SAMPLE PREPARATION

Accessing HCFI for optical analysis generally involves the preparation of thin “wafer like” sections of the sample (19). For rock samples, whole wafers are prepared, whereas with drill core cuttings the material is often comprised of small flakes/chips of rock. For these drill cuttings it is more practical to mount the chips in resin prior to wafer preparation. Unlike conventional rock slabbing where a fast rotating diamond-tipped saw is used to cut through the sample, fluid inclusion saws rotate at much lower revolutions and the sample requires cooling. This is critical because the temperatures generated by these blades can compromise fluid inclusions that have low homogenisation temperatures. A cutting oil is commonly mixed with water to lubricate as well as cool the blade and therefore one should be aware of potential damage to, and contamination of wafers and their inclusions. Spurious apparent HCFI can be created by the lubrication fluid but these false fluorescent targets can usually be recognised by the fact that the fluorescence is localised at the wafer surface. After the first cut is made, the wafer is ground and then polished to generate a good-quality flat surface. Resin can then be applied to the polished surface so that it may be mounted on a glass slide. A second parallel cut is then carefully made to produce a wafer that is several hundred microns in thickness, depending on the thickness required. For high-quality optical measurements thicknesses of ~150 microns are ideal. Grinding and polishing of the new surface results in a doubly-polished wafer that is suitable for microscopic examination. It should be noted that curing of the resin needs to be at low temperature so as to avoid potential HCFI decrepitation (47). For friable samples, McNeil and Morris (48) detail a method that employs resin impregnation into the sample that produces a polyester cast suitable for thin wafer generation. One should, however, take care with the type of resins being used, as many of these can be fluorescent under UV illumination, which can cause problems for fluorescence based analysis methods.

EPIFLUORESCENCE MICROSCOPY

The initial step in recognising HCFI in geologic sections is by observing fluorescence using an epifluorescence microscope with UV illumination. HCFI have apparent (visually judged) fluorescent colours covering the full visible spectrum from blue to red in addition to white. Because the fluorescence of hydrocarbon-based fluids is composition dependent, the

apparent fluorescent colour is used to distinguish different HCFI generations within the same and different wafers. Unfortunately, the human eye lacks the ability to accurately discriminate discrete wavelengths and therefore reporting visual fluorescence colours is at best a qualitative technique, and does not provide quantitative results (20, 49, 50).

The implementation of epifluorescence microscopy for HCFI analysis has to be considered very carefully since we know that emission properties (λ_{max} , intensity, and lifetime) are all very dependant on the excitation wavelength (24). The instrumentation is nonetheless, relatively simple and low cost, requiring a microscope, UV light source (usually a high-pressure Hg lamp, often fitted with a bandpass filter to transmit a specific excitation light wavelength, typically ~366 nm) and a filter-cube arrangement. The filter cube houses a dichroic mirror that is used to direct the UV light onto the sample and the resultant fluorescence to the operator. A barrier filter (commonly 420 nm long pass) prevents harmful UV light being observed by the observer. The quality of this filter is important, because many light oils fluoresce in the violet region, having small Stokes shifts. If the filter is not sufficiently steep edged at the cut off position, then it will either pass some of the excitation light and/or filter out a substantial amount of the petroleum fluorescence, thus distorting the emission spectrum and colour. The detection system is typically visual via binocular tubes, or video/still image recording by digital or analogue sensors. A selected list of studies that have used epifluorescence for the examination of HCFI are provided in Table 1 along with comments (if available) relating to the wavelengths of the excitation source and the range of wavelengths (by filter or spectrometer) sampled from the fluorescence emission. It is important to note the wide variety of excitation wavelengths and different bandpass filters results in the excitation of different populations of fluorophores, generating intrinsically different emission profiles. Furthermore, the fluorescence emission is then sampled in a wide variety of ways using disparate optical configurations in the emission path. This highlights the potential for problems in assessing HCFI fluorescence colour accurately, particularly if only truncated regions of the fluorescence emission are sampled or if the spectra are not corrected for instrument response. Despite this, epifluorescence remains the most broadly used first-pass technique for identifying and establishing the HCFI paragenesis.

Method	Excitation & filters	Observed Wavelength	Reference
Epifluorescence	UV	Not specified	Burruss et al., 1980 (37)
Epifluorescence	UV, 366 nm	Not specified	Burruss, 1983 (8)
Unknown	Unknown	Unknown	Mukhopadhyay & Rullkotter, 1986 (51)
Epifluorescence, Steady state	366 nm (epi) 270-366 nm	Not specified Not specified	McLimans, 1987 (52)
Epifluorescence	Hg lamp	366 nm long pass	Bodnar, 1990 (53)
Epifluorescence	UV	Not specified	Levine et al., 1991 (54)
Epifluorescence	UV	Not specified	Moser et al., 1992 (55)
Epifluorescence	UV	Not specified	Newell et al., 1993 (56)
Epifluorescence	365 nm	430-750 nm	Pironon et al., 1995 (57)
Epifluorescence,	365 nm	430-750 nm	Pironon et al., 1995 (58)
Epifluorescence	UV	Not specified	Parnell et al., 1996 (59)
Epifluorescence	Not specified	Not specified	Xiao et al., 1996 (60)
Epifluorescence	UV	Not specified	George et al., 1997 (61)
Epifluorescence	UV (Not specified)	Not specified	Parnell et al., 1998 (62)
Epifluorescence	UV	Not specified	George et al., 1998 (63)
Epifluorescence	330-380 nm	Not specified	Dutkiewicz et al., 1998 (12)
Epifluorescence	365 nm	450 barrier	O'Reilly et al., 1998 (64)
Epifluorescence	UV	Not specified	Tseng et al., 1999 (65)
Epifluorescence	UV, Not specified	Not specified	Smale et al., 1999 (66)
Epifluorescence	395 nm	440 nm barrier	Rantitsch et al., 1999 (67)

Epifluorescence	UV	Not specified	Parnell et al., 1999 (68)
Epifluorescence	UV (probably 365 nm)	Not specified	Cesaretti et al., 2000 (69)
Epifluorescence	UV	Not specified	Lonnee & Al-Aasm, 2000 (70)
Epifluorescence	UV	Not specified	Marchand et al., 2000 (71)
Epifluorescence	Ref. Pironon 1998	Not specified	Thiéry et al., 2000 (72)
Epifluorescence	UV	Not specified	Parnell et al., 2000 (73)
Epifluorescence	UV (not specified)	Not specified	Middleton et al., 2000 (74)
Epifluorescence	~365 nm, 330-385 nm	420 barrier filter	George et al., 2001 (20)
Epifluorescence	UV (not specified)	Not specified	Lavoie et al., 2001 (75)
Epifluorescence	Hg lamp (330-380 nm)	Nikon UV-2A block, ~420 nm longpass.	Parnell et al., 2001 (21)
Epifluorescence	UV (not specified)	Not specified	Ceriani et al., 2002. (76)
Epifluorescence	UV	Not specified	England et al., 2002 (13)
Epifluorescence	UV	Not specified	Rossi et al., 2002 (77)
Epifluorescence	365 and 410 nm	Not specified	Lisk et al., 2002 (78)
Epifluorescence	366 nm	Not specified	Mauk & Burruss, 2002 (79)
Epifluorescence	Hg lamp – 362 nm	Blue and green filters	Volk et al., 2002 (80)
Epifluorescence	UV (366 nm)	Not specified	Tseng & Pottorf, 2002. (81)
Epifluorescence	UV, 365 nm	Not specified/digital camera	Dutkiewicz, Ridley, et al. 2003 (82)
Epifluorescence	UV	Not specified	Dutkiewicz & Ridley, 2003 (83)
Epifluorescence	UV	Not specified	Dutkiewicz, Volk, et al., 2003 (84)
Epifluorescence	UV	Not specified	Feely & Parnell, 2003 (85)
Epifluorescence	Hg lamp	Not specified	Boles et al., 2004 (86)
Epifluorescence,	365 nm (12 nm bandpass)	397 long pass	Gonzalez-Partida et al., 2003 (10)
Epifluorescence	UV	Not specified	Martinez-Ibarra et al., 2003 (87)
Epifluorescence	Hg lamp	Not specified, photography.	Parnell et al., 2004 (16)
Epifluorescence	UV	Not specified	Dutkiewicz et al., 2004 (88)
Epifluorescence	UV	Not specified, photography	Jonk et al., 2005 (89)
QGF	254 nm	300 – 600 nm	Liu and Eadington, 2005 (34)
Epifluorescence	UV	Not specified	Volk et al., 2005 (90)
Epifluorescence	UV	Not specified	Dutkiewicz et al., 2006 (91)
Epifluorescence	UV	Not specified	Hanks et al., 2006 (92)
Epifluorescence	Not stated	Not specified	Brincat et al., 2006 (93)
Epifluorescence	330-385 nm	Not specified	Rott and Qing, 2006 (94)
Epifluorescence	Blue-light	Not specified	Wierzbicki et al., 2006 (95)
Epifluorescence	UV (Leitz Ortholux II)	Not specified	Wilkinson et al., 2006 (96)
Epifluorescence	365 nm / Hg lamp	420 nm longpass / digital camera	Baron et al., 2007 (97)
Epifluorescence	UV (330–385 nm)	420 nm longpass	Dutkiewicz et al., 2007 (98)
Epifluorescence	365 nm	Not specified	Higgs et al., 2007 (99)
Epifluorescence	340-380 nm	425 nm barrier	Schubert et al., 2007 (100)
Epifluorescence	365 nm	420 longpass	Baron et al., 2008 (101)
Epifluorescence	UV (360–370 nm)	LP400 longpass	Bourdet et al., 2008 (102)

Table 1: Literature survey (not comprehensive) of the use of epifluorescence microscopy for HCFI analysis. What is very clear is lack of consistency in regard to the specific excitation wavelengths used (centre wavelength and bandpass). There is also a lack of information as to the optical configuration (filters etc.) in the emission path.

The fluorescent colours of HCFI have been used as a guide to estimating the maturity and API gravity (a density measurement)[§] of migrating oil (21, 31, 52, 53, 103, 104).

§ API gravity = ((141.5/specific gravity at 15.6°C) – 131.5).

Generally blue fluorescence is associated with oils of high API gravity whereas inclusions with red fluorescence are linked to less mature oils and lower API gravity (20). However, George et al. (3) show that blue fluorescing HCFI have thermal maturities anywhere within the oil window and that fluorescent colours do not have a reliable correlation with maturity. The charge history of a reservoir, based on fluorescent colours, may be misinterpreted owing to the potential colour populations to represent one single event but that slightly different conditions, mineralogical boundaries (3), or inclusion thickness (105) may change the apparent fluorescence colour. Furthermore, the human perception of colour varies from individual to individual, particularly when the fluorescence intensity of the emission from the inclusion is very low. Coupling this human variability with the non-standard equipment used for epifluorescence imaging, demonstrates the need for care in the interpretation of fluorescence colour results between laboratories. Because of these shortcomings, in many cases, the generational data produced by epifluorescence microscopy has to be validated using additional methods such as petrographic studies to elucidate cross-cutting relationships (1, 2, 52, 106) micro-thermometry (2, 100, 107) or fluorescence lifetime measurements (40, 105) to accurately discriminate the different generations of inclusions.

Conventional epifluorescence microscopy has, however, two significant limitations for the accurate analysis of HCFI. First, standard epifluorescence imaging has very poor spatial resolution along the axial direction (through the sample), and as such cannot easily be used for uncovering the precise spatial arrangement of HCFI within a wafer. The out of focus light often blurs the inclusion images making it also very difficult to measure volumes of inclusions accurately. Second, the characterisation of HCFI based on apparent fluorescent colour is very subjective and at best just a qualitative guide. For more accurate and robust analyses one must consider alternate microscopy techniques with higher spatial resolution and spectroscopic methods that yield more comprehensive data about the composition of the petroleum fluids.

HIGH SPATIAL RESOLUTION MICROSCOPY FOR HCFI ANALYSIS.

While most researchers use conventional epifluorescence microscopy for routine HCFI analysis to provide information about their general location within the sample, the precise location of HCFI in space is often uncertain. Furthermore, while volume determinations may be performed by visual estimation, irregular inclusion shapes can generate large errors. There is a need therefore to make use of techniques capable of providing higher spatial resolution particularly in the axial direction from which quantitative volume and intensity information can be extracted. The ideal solution is to use confocal microscopy, and Pawley (108) gives a detailed overview of the area, the specific methods available, and the hardware required. In many cases this drive for higher spatial resolution has been driven by applications in the life sciences. Most universities will now have a minimum of one or more confocal microscopes, which should be easily available to most inclusion researchers.

Conventional Confocal Fluorescence Microscopy:

The high axial resolution in standard confocal microscopy is achieved by the use of high Numerical Aperture (NA) lenses combined with pinholes in the optical path between the sample and the detector. Stray and out-of-focus light is physically rejected whereas light originating from the desired focal plane is allowed to pass to the detector. Typically, the

detector is a single channel (narrow wavelength range) unit, and therefore, to achieve a 2-D image of a target, the excitation laser spot must be scanned (or rastered) across the sample. This can be achieved in a number of ways either by laser scanning using mirrors (Confocal Scanning Laser Microscopy -CSLM), or by moving the sample stage (using piezo-driven units or stepper motors). Either way, a 3-D image stack is generated by acquiring 2-D optical slices through a sample at spacing comparable to the axial resolution, commonly 1-2 μm . These 3-D images can be used to easily discriminate between the fluorescent oil and non-fluorescent host mineral or vapour bubble. This allows both the spatial locations of HCFI to be determined with relatively high accuracy and the volumes of the fluorescent components of the inclusions to be estimated, Figure 2, (109–112). The accuracy of the method is constrained by a number of factors that include the inherent resolution of confocal microscopes (typically $\sim 0.3 \mu\text{m}$ - lateral and $>1.4 \mu\text{m}$ - axial with 488 nm excitation), variations in refractive index of the sample, focal depth effects, and mineral birefringence (111). These factors, coupled with the need to correctly estimate the thresholds for determining fluorescent and non-fluorescent voxels, can lead to significant errors in volume estimation ($\sim 5\%$ according to 102 and 110).

Another factor in determining the accuracy of this method (and HCFI petrographic/spectroscopic analysis in general) is the type of objective lens used. For volume measurements, accuracy is largely determined by axial and lateral resolution and therefore one must use high NA lenses. However, the use of high NA objectives also reduces the effective working distance (typically 150-170 μm) making it difficult to analyse accurately inclusions deeply located within wafers. Aplin (111) used an oil immersion $\times 60$ lens for this initial work, but erred in ascribing the vertical (z-axis) resolution as being $\sim 0.1 \mu\text{m}$ and that it was limited by the stepper motor stage. In fact the vertical resolution is considerably worse than this (most certainly $>0.5 \mu\text{m}$) and limited by the numerical aperture (108). Pironon et al. (110) also used a $\times 60$ oil objective with an NA of 1.4, and estimated an axial resolution of 0.5 μm . It is interesting to note that most studies use 488 nm excitation, whereas many newer confocal systems are equipped with solid state 405 nm laser diodes (102) which can be focussed to a smaller spot size thus potentially improving the accuracy of volume measurements. Kihle (113) used a $\times 100$ oil immersion objective (Olympus D Apo UV, NA =1.3) for spectroscopic measurements but the system was not utilised in a confocal mode. Musgrave et al. (114) used a $\times 40$ glycerine immersion objective (Zeiss Ultrafluar D NA =0.6, working distance of 360 μm) for spectroscopic measurements. For standard epifluorescence imaging and spectral analysis the use of standard air-spaced objectives is widespread, from $\times 40$ (41) to $\times 50$ power (22). Water immersion (WI) lenses have also been employed, Li et al. 2006 used an epiplanneofluor $\times 40$ WI objective (NA = 0.95).

Method	Measurement	Excitation Wavelength	Emission Wavelength	Reference
Confocal	Volume	488 nm laser	520 ± 32 nm	Pironon et al., 1998 (110)
Confocal	Volume	488 nm laser	Not specified	Aplin et al., 1999 (111)
Confocal	Volume	488 nm laser	Not specified	Aplin et al., 2000 (115)
Confocal	Volume	Not specified	Not specified	Swarbrick et al., 2000 (116)
Confocal	Volume	Not specified	Not specified	Thiéry et al., 2002 (117)
Confocal;	Volume	488 nm laser	Not specified	Tseng and Pottorf, 2002 (81).
Multi-photon (Confocal)	Volume	800 nm fs pulsed laser	Schott glass BG39	Stoller et al., 2007 (118)
Structured-light illumination	Morphology	470 – 490 nm; 540 – 550 nm	515 – 550 nm; 575 – 625 nm	Blamey et al., 2008 (119)
Confocal	Volume	405/488 nm laser	Not specified	Bourdet et al., 2008 (102)

Table 2: Selected examples from the literature on the use of confocal microscopy for the three dimensional analysis of hydrocarbon-bearing fluid inclusions.

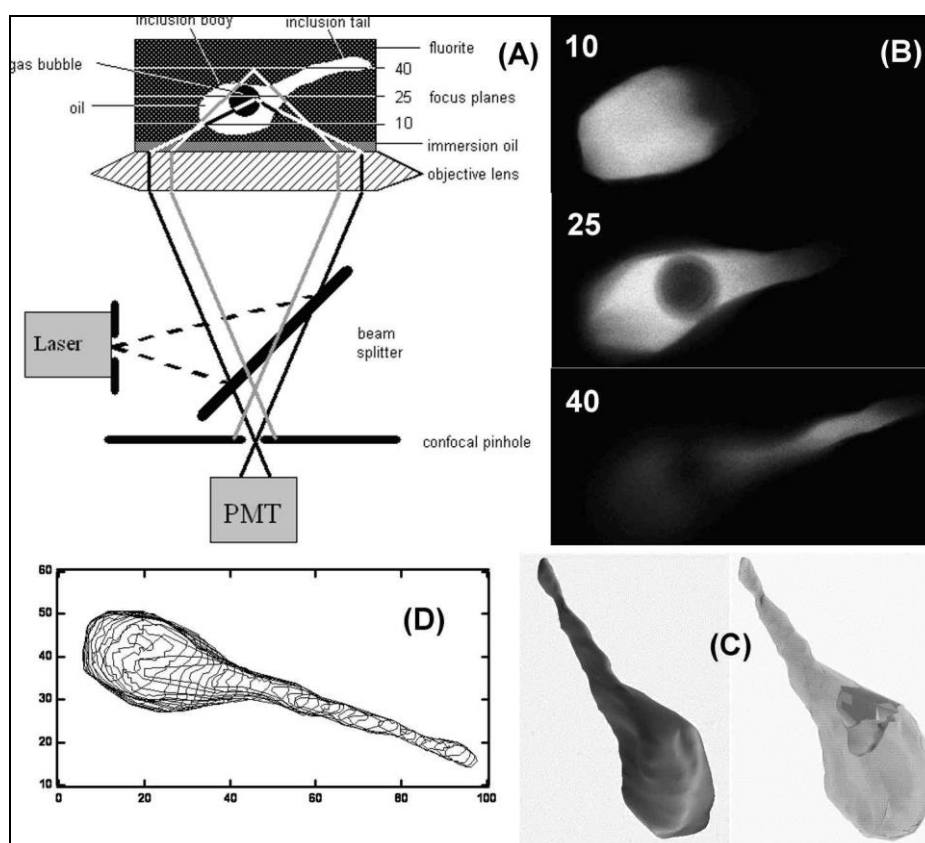


Figure 2: Clockwise from Top Left: Schematic view of the optical path during confocal recording of the image planes of a two-phase oil inclusion; (B) Three two-dimensional CSLM images of the oil inclusion. Two successive planes are separated by 1 µm; (C) 3-D reconstructions of an oil inclusion by surface modelling (GOCAD computer program); a) external surface, b) external surface and vapour-bubble surface in transparency. (D) Superimposed contours of the binarised images of an oil inclusion after thresholding. Scales in micrometer. Adapted from Pironon et al. (110) and reproduced with permission. © *European Journal of Mineralogy*.

Constraining the pressure and temperature conditions during fluid inclusion trapping is highly desirable information for the petroleum exploration industry and can only be

achieved by a combination of homogenisation temperature data and volumetric (Liquid versus vapour bubble ratios i.e. degree of fill.) data (110). Fluid inclusion micro-thermometry, a well established methodology which is described in Roedder (1) and Shepherd et al. (19), is used to generate the homogenisation data. CLSM, can be used to calculate the volume of the vapour and liquid in HCFI by surface modelling and voxel counting (110, 111). By combining the volume estimates with the micro-thermometry data in PVT modelling software, one is able to determine the bulk composition, phase envelope, isochor and some physical properties of the oil as explained by Aplin (111). From examination of several coeval inclusions (inclusions that formed during the same event) it may be possible to obtain information regarding the oil's molar volume, saturation pressure, density, viscosity and surface tension (111). The method is now quite widely used (see Table 2) for examples of routine HCFI analysis.

However, despite it's demonstrated utility for spatial and volume measurements there are some drawbacks associated with standard confocal microscopy. First, the instrumentation in most cases can be very costly and complex, making it an expensive proposition for most geological laboratories. Second, it cannot simultaneously image non-fluorescent Aqueous Fluid Inclusions. Third, most of the potential information in the fluorescence emission is discarded because most CLSM-based methods simply utilise fluorescence intensity as a contrast agent for imaging rather than as an analytical measure of petroleum composition.

Structured-light illumination microscopy:

The Structured-Light Illumination (SLI) technique is a combination of an optical method and computational image analysis that gives comparable results to confocal microscopy by enhancing the axial resolution to provide high-quality optical slices (120). The optical slices may then be merged to create 3-D visualisations of samples such as HCFI. Unlike traditional confocal microscopy, SLI is relatively inexpensive, can have faster acquisition times, and does not require laser excitation sources. Applications to HCFI studies is a relatively new development (119), and it has been shown that SLI microscopy can generate 3-D images of HCFI equivalent to that generated by conventional laser scanning methods. Unlike traditional confocal microscopy methods, an intrinsic characteristic of the methodology also allows for bubbles within aqueous fluid inclusions to be detected and imaged. This allows the pinpointing of the position of aqueous fluid inclusions together with HCFI in the same 3-D visualisation, enabling the rapid and facile determination of paragenetic relationships between HCFI and AFI.

Multi-photon Excitation:

A recent development in fluid inclusion microscopy is the application of second harmonic non-linear effects to the study of aqueous fluid inclusions through the use of pulsed femtosecond lasers (118). The high intensity of the laser pulses generates a very weak second harmonic at the interface between a fluid inclusion and the host mineral that is half the wavelength of the laser's excitation wavelength. In essence, this allows a high resolution confocal-like mapping of the aqueous fluid inclusion's boundaries in 3-D. However, the application of this method for volume measurements to HCFI is not feasible because the generated second harmonic light will induce fluorescence in the petroleum fluid, thus removing the potential for image contrast based on second harmonic light.

These microscopy techniques while providing increased spatial resolution to better view HCFI and the 3-D arrangement within the sample do not generate significant information about the chemical composition of HCFI. In fact these methods tend to discard the valuable information inherent in the fluorescence emission because they only measuring fluorescence at a single wavelength (or at most 2-5 individual wavelengths). To obtain useful information about the chemical composition of the fluids entrapped within the HCFI, one must adapt confocal microscopes for spectroscopic measurements.

MICRO-SPECTROSCOPY OF HCFI.

Extraction of information from the fluorescence emission of HCFI requires the use of various spectroscopic techniques to acquire either steady-state and time-resolved emission parameters. There are no major obstacles to undertaking these types of measurements apart from interfacing the spectroscopic components to the microscope and implementing a rigorous calibration protocol.

Fluorescence emission micro-spectroscopy:

The first obvious step in increasing the discriminating power of fluorescence is to measure the fluorescence emission spectrum. As outlined earlier, heavy (low API gravity) oils have broad, weak, red-shifted emission bands (25, 26, 121) while lighter oils (higher API gravity) tend to have narrower, more intense, and bluer spectra. For spectroscopic measurements, HCFI are illuminated with a monochromatic light source (lamp, laser, or Light Emitting Diode) and the fluorescence intensity as a function of wavelength is measured. There are a number of different hardware approaches that can be taken to make these measurements. In 1994, Musgrave et al., (114) described a home-assembled system using separate lamp and scanning monochromator and photomultiplier tube detector modules. This system was then corrected for non-uniform response across the measured spectrum using a variety of standard samples including uranium glass. It is also possible using fibre optics to couple a standard fluorometer to a microscope (113), thus reducing the complexity of the overall system. Other options include integrated spectrometer/Photomultiplier Tube detector units dedicated for microscopy (31, 100), compact mini-spectrometers with photodiode array detector (41), or more recently Acousto-Optical Tuneable Filter (AOTF) based systems (122). Using a Raman spectrometer (spectrograph with a multi-channel CCD detector) is another option (123, 124) that has been used for HCFI analysis. However, the use of Raman systems for fluorescence studies is typically limited by the fact that the lasers used tend to be visible/NIR (488, 532, 785 nm) rather than UV, thus lowering fluorescence intensity making it more difficult to observe some types of HCFI. Another unhelpful factor is if these visible laser sources are used then the apparent fluorescence colour will be very different than those recorded using UV excitation.

Method/Application	Instrument	Excitation	Emission	Reference
Steady state spectra	Zeiss Zonax	270-366 nm	Unknown	McLimans, 1987 (52)
Lifetime	Unknown	355 nm	400-600 nm	McLimans, 1987 (52)
Steady state spectra	Leitz MPV III	365 nm	430-750 nm Monochromator	Pradier et al. 1990 (33)
Steady state spectra	Leitz MPV III	365 nm	430-750 nm Monochromator	Guilhaumou et al., 1990 (22)
Steady state spectra	Leitz MPV III	365 nm	430-750 nm Monochromator	Pironon and Pradier, 1992 (23)
Synchronous scan	Various (PTI)	Xe lamp, Variable, Monochromator	GG385 long pass & variable, Monochromator	Musgrave et al., 1994 (114)
Steady state excitation and emission spectra	ZEISS, Photomicroscope III	Blue (not specified)	Not specified	Jochum et al., 1995 (125)
FLEEMS (synchronous)	Perkin Elmer LS50 spectrometer	Variable, Monochromator	Variable, Monochromator	Kihle, 1995 (113)
Steady state spectra	Leitz MPV III	365 nm	430-750 nm Monochromator	Pironon et al., 1995 (57)
Steady state spectra	365 nm, filter	Zeiss Ultraviolet G 365 nm excitation filter 420 nm barrier,	400-700 nm (Continuous Filter Monochromator)	Stasiuk and Snowden, 1997 (31)
Steady state spectra	Zeiss II photomicroscope	Hg Lamp; 368 nm filter	400-700 nm	Chi et al., 2000 (126)
Steady state spectra	As per Ref. 31	Not specified	400-700 nm	Lavoie et al., 2001. (75)
Steady state spectra API estimation	Zeiss	Hg lamp; 368 nm filter	400-700 nm 10 nm increments	Kirkwood et al., 2001 (127)
Steady state	Zeiss MPM II	Not specified	400-700 nm	Morrow et al., 2002 (128)
Steady state spectra	Modified Zeiss type Axioplan II microscope	Laser, 360 nm	400-671 nm; OMA 2000 EG&G model 1421	Blanchet et al., 2003 (41)
Steady state spectra	Leitz MPV-III	UV; 365 nm	400-700 nm	Li and Parnell, 2003. (129)
Steady state spectra	Zeiss UMSP 50 spectrometer	Hg lamp (not specified, <395 nm)	395 nm barrier filter; 400-700 nm spectrometer	Alderton et al., 2004 (130)
Steady state spectra	As per Kihle, 1995.	UV, 365 nm	No barrier filter 400-700 nm	Munz et al., 2004 (131)
QGF	QFT-II	254 and 260 nm	300 – 600 nm	Liu and Eadington, 2005 (34)
Steady state spectra	As per Ref. 31	Not specified	Not specified	Lavoie et al., 2005 (132)
Lifetime	PicoQuant & Olympus	405 nm	450-800 nm, monochromator	Ryder et al., 2004 (40)
Steady state spectra	Zeiss Axioplan II microscope	Hg lamp; 365 nm filter	420-720 nm, Zeiss MPM 200/650 photometer and continuous filter monochromator.	Li et al., 2006 (133)

Table 3: Literature survey of spectral methods used for HCFI analysis. What is clearly evident is the wide variation in instrumentation, excitation wavelengths, and detection systems.

Lasers are preferred as excitation sources for microscope based emission spectroscopy because of the very narrow bandpass and long coherence length, which allows for more precise focussing into HCFI. This in turn, ensures that the spectroscopic data is collected only from the inclusion and not from the surrounding mineral. However, to achieve the maximum benefit from laser sources one should make use of confocal optics to obtain the best spatial resolution and minimise spurious signals from the host matrix. Unfortunately, in the fluorescence HCFI studies reviewed here we have been unable to find any such combination in the literature, although most Raman spectroscopy studies of aqueous inclusions routinely make use of confocal optics to improve spatial resolution. It is vital that HCFI studies be precise in regard to the reporting of optical conditions and filters used for HCFI fluorescence analysis so that data can be compared between different laboratories. However, reviewing the literature (Table 3) show that there is generally no consistency between the different inclusion research laboratories.

Another consideration when attempting to measure emission spectra through microscopes, is the need to undertake some form of spectral correction to account for material imperfections, light absorption, and other optical effects in the excitation and emission light paths. A variety of methods have been used, for example Blanchet et al., (41), used the spectral radiance of a reference quartz-iodine lamp illuminating an opal glass which diffuses by transmission according to Lambert's Law (134). Musgrave et al. (114) used a variety of materials including uranium glass, whole crude oil, and pure organic materials as standards. The spectra of these materials were collected using a factory calibrated spectrometer, and then used to correct the data collected on the microscope. Unfortunately no further specific details were provided. Pironon et al. (58) used a LEITZ uranyl glass (no details available) standard to normalize emission flux measurements to calculate Q_{f535} ratios. A black body curve (using a standard tungsten lamp (3100 K) was used as a reference radiator) was used to correct spectra by Li et al. (133). Huang's group used FluoRef™ slides for spectral correction when studying oil generation from kerogens in a diamond anvil cell (44). This last option would be the best for HCFI analysis; however, we cannot find any validation studies on the accuracy of these slides, unlike other fluorescence standard materials (135). It is important to note that spectral calibration is neither routine nor is there an agreed standard, easily implemented method for HCFI analysis.

Despite the assertion of Barres et al., (136), the fluorescence emission spectrum is a useful source of information on petroleum composition. The use of fluorescence spectroscopy for the analysis of HCFI was first briefly mentioned by McLimans in 1987, and detailed reports started to appear in the early 1990's (22, 23). In these early studies, UV lamps (~365 nm centre wavelength) were used to excite the HCFI and the fluorescence spectra were measured using scanning monochromators. Technological advances in spectroscopic hardware and more affordable microscopes have opened this method to more general use since then and several publications are listed in Table 3. As regards a standard method for evaluating the fluorescence emission spectra from HCFI, there is no set procedure. For example Munz et al. (131), collected emission spectra using the same instrumental configuration described by Kihle (113). They correlated peak wavelength with homogenisation temperature and were able to discriminate two types of inclusion on the basis of micro-thermometry and the maximum of the fluorescence emission. The $Q_{R/G}$ (red-green quotient) proposed by Hagemann and Hollerbach in 1986 was first applied to inclusion analysis by Jochum et al. in 1995 (125), however, there are no details provided as to instrument response correction or to the specific excitation wavelength (they say blue light!!).

They did attempt to correlate their data with the data previously collected on bulk oils by Hagemann and Hollerbach (30), however the correlation is tentative at best.

A more detailed study, which sought to correlate crude oil and fluid inclusion $Q_{R/G}$ ratios with chemical composition was published by Stasiuk and Snowdon (31) in 1997. The values of L_{max} and $Q_{R/G}$ was shown to vary with aromatic and saturate content and a red-shift correlated with increasing aromatic and NSO (Nitrogen-Sulphur-Oxygen containing species, i.e. polar fraction) concentrations. The authors also correlated the spectra obtained from HCFI with data collected from crude oils sourced from carrier beds and reservoir rocks of the Upper Devonian Birdbear Formation in Canada. There are several reports of studies which use fluorescence spectral data to estimate the API gravity of the entrapped fluids according to the Stasiuk and Snowdon correlations (126, 127). The Q_{F-535} ratio proposed by Guilhaumou, Szydowski, and Pradier in 1990 has not been widely adopted; most studies in the literature are from the original authors or collaborators (23, 33, 57, 137, 138). As with the other method, the Q_{F-535} ratio decreases as oils become lighter. In the original work (22) the authors were also able to observe changes in fluorescence emission spectra (a red shift and an increase in the emission band width) when inclusions were overheated to 300°C in a pressure cell at ~40 MPa. The experiment shows seems to indicate that the changes in emission were induced by thermal quenching and photochemical reactions, not surprising since the studies involved prolonged UV exposure. Pironon and Pradier, (23), also investigated heating effects on HCFI (both natural and artificial) using fluorescence and observed a similar irreversible red-shift in the emission spectra and an increase in the Q_{F-535} ratio. This indicates that the heating to high temperatures induces a chemical change in the entrapped fluid. The more recent work with diamond anvil cells (42–44) gives a clearer picture with regard to the evolution of petroleum oils from source kerogen and the influence of temperature.

Attempts to better visualise the variations in HCFI fluorescence saw the application of chromaticity diagrams to quantitatively assess fluorescence colour using data obtained from fluorescence spectra. The analysis of fluorescence colour variations can be improved by plotting the CIE (International Commission on Illumination 1971 (139), 1986 (140)) chromaticity coordinates obtained from fluorescence spectra on a bivariate graph. Segments of the graph are subdivided on the basis of colour and thus the method offers an improvement over purely visual characterisation of colours by individuals. Hagemann and Hollerbach in 1986 plotted spectral data from crude oils onto CIE diagrams while McLimans (52) demonstrated the analysis of single inclusions where the spectral data collected using 366 nm excitation and a Zeiss Zonax system. Specific details of the hardware are scanty but it seems to have been a reflectance measurement system. The information garnered from this type of analysis, indicated that as the oils increase in maturity the x and y co-ordinates decrease, i.e. the fluorescence emission moves towards the blue corner of the graph. Further examples of crude oils and HCFI that have been analysed using these diagrams and comments on the method are detailed by Oxtoby (49), Alderton (130), and Schubert (100). Blanchet et al. (41) give a detailed analysis of fluid inclusions from the North Sea and calibration oils using CIE diagrams. They observed that the fluorescence colour of inclusion oils is variable even within a single fluid inclusion assemblage and they advanced a number of explanations for this based on geological processes. There could have been a progressive entrapment of oil with API gravity increasing through time, or fractionation of the original petroleum fluid could have occurred. Alternatively, since the HCFI occur mostly at grain-overgrowth boundaries and rarely within overgrowths, this could be attributed to the weakness and permeability of the interface, which would infer that the trapping of secondary fluids is possible. Their results also demonstrated that there were significant differences between the

fluorescence colour of the inclusion oils and present-day reference oils. This “red shift” is probably due to the loss of very light hydrocarbon fractions in the reference oils compared to the inclusion trapped oils. However, Blanchet (41) states that this loss of light fraction has no effect, but crucially the reference cited to support this claim has not been published or subjected to peer-review (141). This contention is in direct opposition to the observations made when crude oils are diluted (25, 26, 29, 142).

Figure 3 shows an example of the CIE method applied to HCFI analysis which depicts a well-defined evolution in the fluorescence emission from successive hydrocarbon generations in a sample (SzD-11). For example, the CIE diagram, Fig. 3d plots the early primary inclusions (HC1_L) in a narrow field ($x=0.3$ to 0.34 , $y=0.35$ to 0.4), while the slightly younger intermediate primary inclusions (HC2_L) show a slight red-shift ($x=0.35$ to 0.4 , $y=0.38$ to 0.43) along the McLimans maturity curve (103). The late-primary inclusions (HC3_L) are widely scattered along the same trend ($x=0.29$ to 0.5 , $y=0.36$ to 0.46), indicating a more heterogeneous oil composition. The secondary HC4_L (from SzD-11) inclusions have a narrow range between $x=0.25$ to 0.3 and $y=0.35$ to 0.4 , similar to other HC4_L inclusions sourced elsewhere in the Szeghalom Dome region (Fig. 3e). This example shows how the CIE method can be used for discriminant analysis of multiple inclusion generations across a relatively large geographical location.

In summary, one can see that emission spectroscopy is reasonably well established methodology for HCFI analysis, but that it suffers from the use of a wide diversity of instrumentation and variances in specific methods. This makes it difficult to compare data between different laboratories. This seems to have arisen from the historical use of home-built apparatus and the relative costs of the instrumentation required. However, with the recent advent of low cost, reliable UV and violet (375 and 405 nm) solid state lasers and integrated CCD based spectrometers, one could suggest the possibility for developing and implementing a standard HCFI measurement and analysis methodology based on fluorescence spectroscopy.

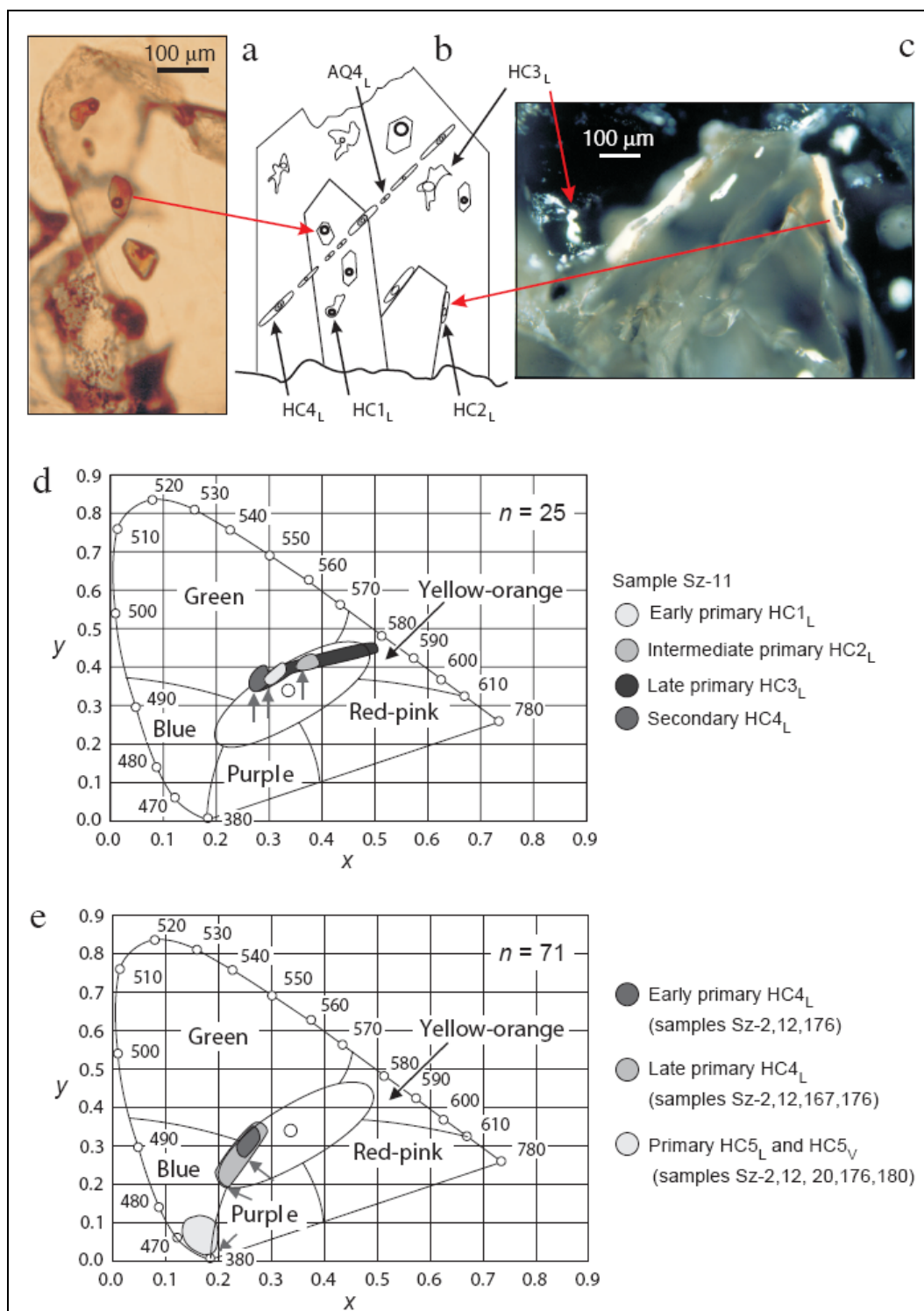


Figure 3: (a) Early idiomorphic crystal of quartz from the Sz-11 well, containing primary HC1_L inclusions, viewed in plane-polarized transmitted light. (b) Schematic petrographic relationships: fluid generations 1 to 3 are represented by a succession of primary inclusions (HC1_L, HC2_L to HC3_L). Fluid generation 4 is represented by coexisting petroleum (HC4_L) and aqueous (AQ4_L) inclusions in a healed fracture. (c) Example of HC2_L and HC3_L inclusions viewed in UV epi-illumination. (d) UV-fluorescence colours of 25 inclusions from sample Sz-11, plotted in the CIE-1931 chromaticity diagram. Each petroleum generation displays slightly different colours. (e) UV-fluorescence colours of 71 primary HC4_L, HC5_L and HC5_V petroleum inclusions from various samples, displayed in the CIE-1931 chromaticity diagram. Reprinted with permission from *Chemical Geology*, Reference 100, © 2007, Elsevier.

Fluorescence excitation-emission matrix (EEM) spectroscopy:

Unlike epifluorescence and steady-state emission spectroscopy where narrow band or monochromatic UV light is employed, for multidimensional fluorescence measurements like total synchronous fluorescence scanning (TSFS) or excitation-emission matrix (EEM) spectroscopy, a series of excitation wavelengths are used from the UV to the visible region of the spectrum. The rationale behind the use of EEM and TSFS is that these measurements explore the complete emission space, producing a map of the effect of excitation wavelength on emission properties from which energy transfer processes can be observed (143, 144). Light oils have relatively narrow, intense fluorescence emission bands with small Stokes' shifts in comparison to heavy oils where the emission band tends to be weaker, broader, and red shifted (143). For the instrumentation required one can either develop a home built system with emission and excitation monochromators (114) or combine a standard fluorometer to a microscope using fibre optics (113). For EEM measurements, the emission spectrometer is scanned over a defined emission wavelength range for a series of excitation wavelengths. In contrast TSFS measurements involve the synchronous scanning of the excitation and emission monochromators at a variety of fixed wavelength separations (113). In both cases the excitation source is typically a Xenon lamp which provides a stable light output from the UV into the visible. Studies of HCFI using this technique have shown the ability to discriminate different HCFI populations based on the quantitative parameters of optimum excitation wavelength, optimum emission wavelength, and Stokes' shift (113). However, despite the high information content in EEM or TSFS spectra the method has not been widely adopted for inclusion studies. This is probably due to the relatively high cost of the equipment, complexity of integration, difficulties in signal calibration and correction, and the difficulty in easily analysing the complex data generated. EEM and TSFS data is very sensitive to the collection conditions and there are no defined standard methods as yet for signal correction in microscopy systems.

The main disadvantages of steady-state spectroscopic methods for HCFI analysis are: the lack of standardisation, the difficulty in obtaining absolute intensity values and corrected emission spectra, the negative impacts of sample turbidity and opaqueness, and the possibility of photobleaching/photoalteration (23) if long exposure times are used with UV excitation (20, 24, 145). The measurement of absolute emission intensities can be compounded by fluctuations in excitation source, detector electronics, photobleaching, sample turbidity, and absorption characteristics of the host mineral (24). Most fluorescence measurements are made in a single channel mode and therefore do not include a reference channel. Therefore implementation of reference measurements in order to acquire accurate intensity based measurements is often a time-consuming process particularly when dealing with complex samples such as HCFI. An additional and significant problem lies in the wide variety of optical configurations that have been used for spectroscopic analysis (Table 2). This multiplicity of the optical configurations can lead to alterations in the true emission spectra owing to irregularities in the absorption and reflection of optical emission, interference, and dichroic filters. These factors are much less constricting when working with time-resolved measurements, particularly fluorescence lifetimes, where the lifetime is largely independent of the emission intensity.

Fluorescence Lifetime Microscopy (FLIM):

The fluorescence lifetime of a molecule can be regarded as the average time it spends in the excited state after absorbing a photon of light. For individual molecules in dilute solutions the lifetimes can easily be ascribed to specific excited states, and one can correlate lifetime changes with specific environmental factors (146). The factors that influence the experimentally measured value of the lifetime include molecular structure, environment, fluorophore concentration, and interacting species concentrations. In the context of complex fluids like petroleum, the interacting species can be divided into two broad classes, those which cause fluorescence quenching (non-radiative), and those that promote energy transfer which results in radiative processes like emission (147). The radiative processes are largely determined by molecular structure and energy transfer, whereas the non-radiative processes are largely governed by collisional, static, and sphere of action quenching. On average, heavy oils (low API gravity) have shorter average lifetimes than light oils (28, 29, 147, 148). The average fluorescence lifetime also depends on the specific emission wavelength because different regions of the emission spectrum represent different populations of emitting fluorophores. The excitation wavelength also affects the average lifetime with a reduction in lifetime occurring as the excitation wavelength increases (24, 28, 29). Qualitative correlations of fluorescence lifetime data with compositional parameters such as API gravity, polar concentrations, and corrected alkane concentrations have been reported (28, 40, 121, 147). Although accurate quantitative correlations have not been possible with fluorescence lifetimes, the method can be exploited for the accurate characterisation and discrimination of different petroleum oil types, particularly when trapped in HCFI.

There are two principal methods of measuring average fluorescence lifetimes, they are by the time domain (TD) and frequency domain (FD) methods (146). In TD, a pulsed laser is used as the excitation source and the fluorescence decay is measured by either a Time Correlated Single Photon Counting (TCSPC) detection system (28, 146), or a time-gated camera (149), or a streak camera (150). A real decay profile (a combination of the Instrument Response Function (IRF) and the sample fluorescence decay) is generated that enables the fluorescence lifetime to be recovered by various mathematical deconvolution procedures. However, accurate deconvolution and recovery of fluorescence lifetimes requires the collection of an IRF which is typically a non-fluorescent scattering sample like Ludox. It is important that the IRF be collected using the same optical path length and conditions as for the sample measurement. The deconvolution of the decay curve can be accomplished using a variety of different models, depending on the sample under investigation. For simple mixtures (1-4 fluorophores), discrete lifetimes can be extracted, while for more complex situations (e.g. where a single fluorophore exists in multiple environments) lifetime distribution models (Gaussian, Lorentzian, or stretched exponentials) can be used. However, for complex fluids like crude petroleum oil it has been found experimentally that it is best to report the intensity averaged lifetime (121). Coupling TCSPC to microscopes for measurement of lifetimes from HCFI is straightforward (151) and now there are many commercial systems available either for retrofitting to existing microscopes or as complete integrated systems.

FD measurement methods now normally use laser or Light Emitting Diode (LED) excitation where the output is modulated with a sinusoidal waveform and phase sensitive detection of the fluorescence emission (146). The modulated excitation generates a modulated fluorescence emission from the sample at the same frequency, but which is

demodulated and phase shifted with respect to the input according to the fluorescence lifetime. For nanosecond lifetimes in the 100 to ~1 ns range modulation frequencies of 1 to 500 MHz range can be used. As the lifetimes decrease below ~1 ns it is advantageous to use frequencies in the GHz range (146). For accurate lifetime measurements of complex systems which contain more than one fluorophore, one must measure the phase and demodulation data at a range of frequencies and then fit the data to extract the lifetime information. In the case of crude oils, 40 frequencies are typically required (152) to obtain reliable and reproducible lifetime data. On the other hand, if one simply needs to rapidly discriminate oils of different lifetime one can use a single modulation frequency. The FD principle has also been applied to standard epifluorescence wide field imaging (153) to produce a methodology capable of rapid FLIM imaging. More recent developments have coupled this with spinning disc technologies to deliver rapid confocal-FLIM (154). However, to date (mid 2008) there have been no reports of its use for HCFI studies. FD has an advantage over TD in that no deconvolution is required to calculate the lifetime. However, unlike the TD method, fluorescent standards of precisely known lifetime are needed to calibrate the phase-shift and demodulation scales (155). In practical terms when studying crude petroleum oils or HCFI where there are large variations in lifetime with emission wavelength there is a need to employ several calibration standards (152, 156, 157). Another factor which is particularly relevant to HCFI studies is the need to acquire the calibration data with similar fluorescence intensities to that being measured from the sample (155). It should also be noted that the standards currently used, are usually solutions of organic fluorophores with well defined single-exponential lifetimes, so care needs to be exercised to ensure that fresh solutions are used, and that the lifetimes are validated using TCSPC or equivalent measurements.

When comparing FD versus TD methods for HCFI analysis there are pros and cons for each method. One significant disadvantage of the FD methods is that the technique is much less sensitive than TCSPC, and therefore requires that the HCFI be illuminated at relatively higher light intensities and for longer periods of time. On the other hand, the method (in single frequency mode) is very rapid for imaging purposes, suitable for initial screening of HCFI. Another advantage of the FD procedure is that no deconvolution is required, making data analysis comparatively rapid. Measuring fluorescence lifetimes using TD methods requires the use of fast pulsed lasers and sophisticated detection electronics or detectors. This contributes to overall system cost and complexity, and while TCSPC systems have become more economical, robust, and very easy to use, TD lifetime systems are still relatively expensive. The correlation between frequency domain and time domain measurements for crude oil lifetimes has been carefully evaluated (152). The study indicated that the choice of model (discrete, Lorentzian or Gaussian) used to calculate the average lifetime is very important in both TD and FD methods.

There are several advantages of fluorescence lifetime measurements over conventional epifluorescence imaging or steady-state emission measurements. Fluorescence lifetime measurements are much less sensitive to source and detector fluctuations, light scattering, mineral absorption, and photobleaching than other techniques. In addition, the measurement is quantitative, repeatable, and easily validated using lifetime standards available for nearly all emission and excitation wavelengths to be used for HCFI analysis (146). When lifetime measurements are implemented in confocal microscopes, measurements can easily be made on HCFI as small as 1 μm . McLimans in 1987 suggested the potential in using time-resolved spectroscopy for the analysis of HCFI. Data was presented showing a tentative negative correlation between maturity and fluorescence lifetime for several crude oils. However, this correlation does not match the observations of

any subsequent studies where it is clear that the fluorescence lifetime increases with increasing API gravity and maturity (28, 29, 40, 121, 147, 152). However, McLimans did not present any data collected from HCFI in this 1987 publication. To the best of our knowledge the first detailed reports of fluorescence lifetime measurements on HCFI were published by our group in Galway (40, 158, 159). These studies presented lifetime data for both crude petroleum oils and HCFI, measured using the TCSPC method. The key observation was that many of the HCFI demonstrated significantly longer average fluorescence lifetimes than the calibration oils studies, indicating that the dilution effect arising from the light hydrocarbons still present in the trapped inclusion fluids have a significant impact on emission properties.

For discriminating between multiple HCFI assemblages, one can use FLIM in a number of different modes. First, for the rapid screening of HCFI (and generation of FLIM images), the fluorescence lifetime can be measured over a wide emission range (typically using just a longpass filter) to yield a single lifetime value (105, 107, 157). These single lifetime value measurements, using 405 nm excitation, have been used to discriminate multiple HCFI generations within the same HCFI sample (105). This measurement mode also has the advantage of using all the emission light, so can be used to measure weakly emitting HCFI. Second, lifetimes can be measured at a range of discrete emission wavelengths. Lifetime-wavelength (τ - λ) plots can then be generated for the accurate discrimination of closely related petroleum fluids (40, 107). This however relies on the collection of data at a range of wavelengths (using monochromator or filters) and is therefore relatively slow.

CONCLUDING REMARKS:

The study of Hydrocarbon-bearing Fluid Inclusions (HCFI) is important from a geologic viewpoint because it offers a unique insight into the formation and development of petroleum basins. A combination of the relative chronology of inclusions (both aqueous and HCFI) as well as the composition and temperature-pressure-volume characteristics of individual inclusions provides valuable information about the thermal history and migration of hydrocarbons in petroleum basins (1). Understanding these mechanisms that ultimately result in the creation of economic recoverable crude oil is vital to petroleum exploration because it provides predictive models and key indicators that may lead to further discoveries or to better reservoir management.

The use of fluorescence microscopy and spectroscopy in a wide variety of methodologies for the characterization and analysis of HCFI is well established. The petroleum fluids entrapped in HCFI fluoresce because of the presence of polycyclic aromatic hydrocarbons. However, it is the complex chemical composition of the entrapped oils ultimately determines the precise absorption and fluorescence characteristics of HCFI. HCFI analysis by fluorescence can be subdivided into two main categories, first estimating the hydrocarbon composition and second, establishing spatial relationships between and volumes within HCFI. HCFI composition can be estimated (with varying degrees of accuracy) from a variety of emission parameters including colour, chromaticity diagrams, Stokes shifts, emission fluxes, emission intensity ratios, and fluorescence lifetimes. Confocal Microscopy allows for the facile determination of the spatial arrangement, relationships, and volumes of HCFI. This spatial information yields valuable data regarding the timing between HCFI assemblage formation, while the volume estimates of the internal phases, combined with

microthermometry, provides information regarding density, pressure and temperature at the time of trapping.

However, there are problems with the use of fluorescence methods, particularly in the areas of instrumentation, calibration, and validation. The variety of instrumentation and protocols used make it difficult to accurately compare results from various laboratories. This is compounded by the lack of a set of petroleum oils and HCFI standards, suitable for both instrument calibration and validation. A set of petroleum oils with which one can produce an accurate and reproducible calibration plot for estimating HCFI composition is of particular importance. A wide variety of very disparate petroleum oils have been used by different research groups to generate different calibration plots, based on different emission parameters, recorded on different instrumentation, and this compromises the utility of the data. The development of standard methods (defined excitation wavelengths, emission optics, and instrument calibration protocol) suitable for implementation in any inclusion laboratory should also be explored. In conclusion, while fluorescence provides a very powerful and effective tool for the analysis of fluid inclusions, there is still scope for much improvement.

ACKNOWLEDGEMENTS:

This research was funded by the Science Foundation of Ireland's Research Frontiers Programme Grant (05/RFP/GEO0002).

REFERENCES:

1. E. Roedder, Fluid Inclusions. Mineralogical Society of America. *Reviews in Mineralogy*, **12**, 1-644, (1984).
2. I.A. Munz, Petroleum inclusions in sedimentary basins: systematics, analytical methods and applications. *Lithos*, **55**(1-4), 195-212, (2001).
3. S.C. George, H. Volk, and M. Ahmed, Geochemical analysis techniques and geological applications of oil-bearing fluid inclusions, with some Australian case studies. *J. Petrol. Sci. Eng.*, **57**(1-2), 119-138, (2007).
4. I.A. Munz, K. Iden, H. Johansen, and K. Vagle, The fluid regime during fracturing of the Embla field, Central Trough, North Sea. *Mar. Pet. Geol.*, **15**(8), 751-768, (1998).
5. O. Walderhaug, Temperatures of quartz cementation in Jurassic sandstones from the Norwegian continental shelf—evidence from fluid inclusions. *Journal of Sedimentary Petrology*, **64**(2), 311–323, (1994).
6. O. Walderhaug, and P.A. Bjorkum, The Effect of Stylolite Spacing on Quartz Cementation in the Lower Jurassic Stø Formation, Southern Barents Sea. *J. Sediment. Res.*, **73**(2), 146-156, (2003).
7. N.H. Oxtoby, A.W. Mitchell, and J.G. Gluyas, The filling and emptying of the Ula Oilfield: fluid inclusion constraints. In: *The geochemistry of reservoirs: Special Publication*, (Eds. Cubitt, J. M., and England, W. A.), Geological Society, London, **86**, 141-157, (1995).
8. R.C. Burruss, K.R. Cercone, and P.M. Harris, Fluid inclusion petrography and tectonic-burial history of the Al Ali No. 2 well; evidence for the timing of diagenesis and oil migration, northern Oman Foredeep. *Geology*, **11**(10), 567-570, (1983).
9. J. Jensenius and R.C. Burruss, Hydrocarbon-water interactions during brine migration: Evidence from hydrocarbon inclusions in calcite cements from Danish North Sea oil fields. *Geochim. Cosmochim. Acta*, **54**(3), 705-713, (1990).
10. E. Gonzalez-Partida, A. Carrillo-Chavez, J.O.W. Grimmer, J. Pironon, J. Mutterer, and G. Levresse, Fluorite deposits at Encantada-Buenavista, Mexico: products of Mississippi Valley type processes. *Ore Geol. Rev.*, **23**(3-4), 107-124, (2003).

11. M.A. Kendrick, R. Burgess, R.A.D. Patrick, and G. Turner, Hydrothermal fluid origins in a fluorite-rich Mississippi Valley-Type district: Combined noble gas (He, Ar, Kr) and halogen (Cl, Br, I) analysis of fluid inclusions from the South Pennine Ore Field, United Kingdom. *Econ. Geol.*, **97**(3), 435-451, (2002).
12. A. Dutkiewicz, B. Rasmussen, and R. Buick, Oil preserved in fluid inclusions in Archaean sandstones. *Nature*, **395**, 885-888, (1998).
13. G.L. England, B. Rasmussen, B. Krapez, and D.I. Groves, Archaean oil migration in the Witwatersrand Basin of South Africa. *J. Geol. Soc.*, **159**(2), 189-201, (2002).
14. B. Rasmussen, Evidence for pervasive petroleum generation and migration in 3.2 and 2.63 Ga shales. *Geology*, **33**(6), 497-500, (2005).
15. V. Lüders and K. Rickers, Fluid inclusion evidence for impact-related hydrothermal fluid and hydrocarbon migration in Cretaceous sediments of the ICDP-Chicxulub drill core Yax-1. *Meteorit. Planet. Sci.*, **39**(7), 1187-1197, (2004).
16. J. Parnell, G.R. Watt, D. Middleton, J. Kelly, and M. Baron, Deformation band control on hydrocarbon migration. *J. Sediment. Res.*, **74**(4), 552-560, (2004).
17. J.M. Peter, B.R.T. Simoneit, O.E. Kawka, and S.D. Scott, Liquid hydrocarbon-bearing inclusions in modern hydrothermal chimneys and mounds from the southern trough of Guaymas Basin, Gulf of California. *Appl. Geochem.*, **5**(1-2), 51-63, (1990).
18. J.M. Hunt, *Petroleum Geochemistry and Geology*. W.H. Freeman and Company, San Francisco, (1979).
19. T.J. Shepherd, A.H. Rankin, and D.H.M. Alderton, *A Practical Guide to Fluid Inclusion Studies*, Blackie and Son, Glasgow, (1985).
20. S.C. George, T.E. Ruble, A. Dutkiewicz, and P.J. Eadington, Assessing the maturity of oil trapped in fluid inclusions using molecular geochemistry data and visually-determined fluorescence colours. *Appl. Geochem.*, **16**(4), 451-473, (2001).
21. J. Parnell, D. Middleton, C. Honghan, and D. Hall, The use of integrated fluid inclusion studies in constraining oil charge history and reservoir compartmentation: examples from the Jeanne d'Arc Basin, offshore Newfoundland. *Mar. Pet. Geol.*, **18**(5), 535-549, (2001).
22. N. Guilhaumou, N. Szydłowski, and B. Pradier, Characterization of hydrocarbon fluid inclusions by infra-red and fluorescence microspectroscopy. *Mineral. Mag.*, **54**(375), 311-324, (1990).
23. J. Pironon and B. Pradier, Ultraviolet-Fluorescence alteration of hydrocarbon fluid inclusions. *Org. Geochem.*, **18**(4), 501-509, (1992).
24. A.G. Ryder, Analysis of crude petroleum oils using fluorescence spectroscopy. In: C.D. Geddes and J.R. Lakowicz, Editors, *Reviews in Fluorescence 2005*, Springer (2005) pp. 169-198.
25. T.D. Downare and O.C. Mullins, Visible and near-infrared fluorescence of crude oils. *Appl. Spectrosc.*, **49**(6), 754-764, (1995).
26. C.Y. Ralston, X. Wu, and O.C. Mullins, Quantum yields of crude oils. *Appl. Spectrosc.*, **50**(12), 1563-1568, (1996).
27. O.C. Mullins and E.Y. Sheu, *Structure and Dynamics of Asphaltenes*, Plenum Press, New York, 21-77, (1998).
28. A.G. Ryder, T.J. Glynn, M. Feely, and A.J.G. Barwise, Characterization of crude oils using fluorescence lifetime data. *Spectrochim. Acta (A)*, **58**(5), 1025-1038, (2002).
29. X. Wang and O.C. Mullins, Fluorescence lifetime studies of crude oils. *Appl. Spectrosc.*, **48**(8), 977-984, (1994).
30. H.W. Hagemann and A. Hollerbach, The fluorescence behaviour of crude oils with respect to their thermal maturation and degradation. *Org. Geochem.*, **10**(1-3), 473-480, (1986).
31. L.D. Stasiuk and L.R. Snowdon, Fluorescence micro-spectrometry of synthetic and natural hydrocarbon fluid inclusions: crude oil chemistry, density and application to petroleum migration. *Appl. Geochem.*, **12**(3), 229-241, (1997).
32. L.D. Stasiuk, T. Gentzis, and P. Rahimi, Application of spectral fluorescence microscopy for the characterization of Athabasca bitumen vacuum bottoms. *Fuel*, **79**(7), 769-775, (2000).
33. B. Pradier, C. Largeau, S. Derenne, L. Martinez, P. Bertrand, and Y. Pouet, Chemical basis of fluorescence alteration of crude oils and kerogens--I. Microfluorimetry of an oil and its isolated fractions; relationships with chemical structure. *Org. Geochem.*, **16**(1-3), 451-460, (1990).
34. K.Y. Liu and P. Eadington, Quantitative fluorescence techniques for detecting residual oils and reconstructing hydrocarbon charge history. *Org. Geochem.*, **36**(7), 1023-1036, (2005).
35. S. Gong, S.C. George, H. Volk, K. Liu, and P. Peng, Petroleum charge history in the Lunnan low uplift, Tarim basin, China - Evidence from oil-bearing fluid inclusions. *Org. Geochem.*, **38**(8), 1341-1355, (2007).
36. R.C. Murray, Hydrocarbon Fluid Inclusions in Quartz. *Amer. Assoc. Pet. Geol. Bull.* **41**(5), 950-956, (1957).

37. R.C. Burruss, D.J. Toth, and R.H. Goldstein, Fluorescence microscopy of hydrocarbon fluid inclusions: relative timing of hydrocarbon migration events in the Arkoma Basin, NW Arkansas. *EOS* **61**, 400, (1980).
38. R.C. Burruss, Hydrocarbon fluid inclusions in studies of sedimentary diagenesis. *Mineral. Assoc. Canada, Short Course Handbook* 6, 138-156, (1981).
39. R.C. Burruss, Practical aspects of fluorescence microscopy of petroleum fluid inclusions. Luminescence microscopy and spectroscopy: Qualitative and quantitative applications. In: Barker, C.E., and Kopp, O.C. (Eds.), *SEPM Short Course* 25, 1-7, (1991).
40. A.G. Ryder, M.A. Przyjalowski, M. Feely, B. Szczupak, and T.J. Glynn, Time-resolved fluorescence microspectroscopy for characterizing crude oils in bulk and hydrocarbon bearing fluid inclusions. *Appl. Spectrosc.*, **58**(9), 1106-1115, (2004).
41. A. Blanchet, M. Pagel, F. Walgenwitz, and A. Lopez, Microspectrofluorimetric and microthermometric evidence for variability in hydrocarbon fluid inclusions in quartz overgrowths: implications for inclusion trapping in the Alwyn North field, North Sea. *Org. Geochem.*, **34**(11), 1477-1490, (2003).
42. W.-L. Huang and G.A. Otten, Cracking kinetics of crude oil and alkanes determined by diamond anvil cell-fluorescence spectroscopy pyrolysis: technique development and preliminary results. *Org. Geochem.*, **32**(6), 817-830, (2001).
43. R.-F. Weng, W.-L. Huang, C.-L. Kuo, and S. Inan, Characterization of oil generation and expulsion from coals and source rocks using diamond anvil cell pyrolysis. *Org. Geochem.* **34**(6), 771-787, (2003).
44. Y.-J. Chang and W.-L. Huang, Simulation of the fluorescence evolution of "live" oils from kerogens in a diamond anvil cell: Application to inclusion oils in terms of maturity and source. *Geochim. Cosmochim. Acta*, **72**(15), 3771-3787, (2008).
45. J. Kihle and H. Johansen, Low-temperature isothermal trapping of hydrocarbon fluid inclusions in synthetic-crystals of KH_2PO_4 . *Geochim. Cosmochim. Acta*, **58**(3), 1193-1202, (1994).
46. S. Teinturier, M. Elie, and J. Pironon, Oil-cracking processes evidence from synthetic petroleum inclusions. *J. Geochem. Explor.*, **78-79**, 421-425, (2003).
47. A.M. Van den Kerkhof and U.F. Hein, Fluid inclusion petrography. *Lithos*, **55**(1-4), 27-47, (2001).
48. B. McNeil and E. Morris, The Preparation of Double-Polished Fluid Inclusion Wafers from Friable, Water-Sensitive Material. *Mineralogical Magazine*; **56**(382), 120-122, (1992).
49. N.H. Oxtoby, Comments on: Assessing the maturity of oil trapped in fluid inclusions using molecular geochemistry data and visually-determined fluorescence colours. *Appl. Geochem.*, **17**(10), 1371-1374, (2002).
50. S.C. George, T.E. Ruble, A. Dutkiewicz, and P.J. Eadington, Reply to comment by Oxtoby on "Assessing the maturity of oil trapped in fluid inclusions using molecular geochemistry data and visually-determined fluorescence colours". *Appl. Geochem.*, **17**(10), 1375-1378, (2002).
51. P.K. Mukhopadhyay and J. Rullkotter, Quantitative microscopic spectral fluorescence measurement of crude oil, bitumen, kerogen and coal. *AAPG Bull.*, **70**(5), 624, (1986).
52. R.K. McLimans, The application of fluid inclusions to migration of oil and diagenesis of in petroleum reservoirs. *Appl. Geochem.*, **2**(5-6), 585-603, (1987).
53. R.J. Bodnar, Petroleum migration in the Miocene Monterey Formation, California, USA: constraints from fluid inclusion studies. *Mineral. Mag.*, **54**(375), 295-304, (1990).
54. J.R. Levine, I.M. Samson, and R. Hesse, Occurrence of fracture-hosted impsonite and petroleum fluid inclusions, Quebec City region, Canada. *AAPG Bull.*, **75**(1), 139-155, (1991).
55. M.R. Moser, A.H. Rankin, and H.J. Milledge, Hydrocarbon-bearing fluid inclusions in fluorite associated with the Windy Knoll Bitumen Deposit, UK. *Geochim. Cosmochim. Acta*, **56**(1), 155-168, (1992).
56. K.D. Newell, R.C. Burruss, and J.G. Palacas, Thermal maturation and organic richness of potential petroleum source rocks in Proterozoic Rice Formation, North American Mid-Continent Rift System, northeastern Kansas. *AAPG Bull.*, **77**(11), 1922-1941, (1993).
57. J. Pironon, M. Pagel, M.H. Leveque, and M. Moge, Organic inclusions in salt .1. Solid and liquid organic-matter, carbon-dioxide and nitrogen species in fluid inclusions from the Bresse Basin (France). *Org. Geochem.*, **23**(5), 391-402, (1995).
58. J. Pironon, M. Pagel, F. Walgenwitz, and O. Barres, Organic inclusions in salt .2. Oil, gas and ammonium in inclusions from the Gabon Margin. *Org. Geochem.*, **23**(8), 739-750, (1995).
59. J. Parnell, P.F. Carey, and B. Monson, Fluid inclusion constraints on temperatures of petroleum migration from authigenic quartz in bitumen veins. *Chem. Geol.*, **129**(3-4), 217-226, (1996).
60. X.M. Xiao, D.H. Liu, and J.M. Fu, Multiple phases of hydrocarbon generation and migration in the Tazhong petroleum system of the Tarim Basin, People's Republic of China. *Org. Geochem.*, **25**(3-4), 191-197, (1996).

61. S.C. George, F.W. Krieger, P.J. Eadington, R.A. Quezada, P.F. Greenwood, L.I. Eisenberg, P.J. Hamilton, and M.A. Wilson, Geochemical comparison of oil-bearing fluid inclusions and produced oil from the Toro Sandstone, Papua New Guinea. *Org. Geochem.*, **26**(3-4), 155-173, (1997).
62. J. Parnell, P. Carey, and W. Duncan, History of hydrocarbon charge on the Atlantic margin: Evidence from fluid-inclusion studies, West of Shetland. *Geology*, **26**(9), 807-810, (1998).
63. S.C. George, M. Lisk, R.E. Summons, and R.A. Quezada, Constraining the oil charge history of the South Pepper oilfield from the analysis of oil-bearing fluid inclusions. *Org. Geochem.*, **29**(1-3), 631-648, (1998).
64. C. O'Reilly, P.M. Shannon, and M. Feely, A fluid inclusion study of cement and vein minerals from the Celtic Sea Basins, offshore Ireland. *Mar. Pet. Geol.*, **15**(6), 519-533, (1998).
65. H.-Y. Tseng, R.C. Burruss, T.C. Onstott, and G. Omar, Paleofluid-flow circulation within a Triassic rift basin: Evidence from oil inclusions and thermal histories. *Geo. Soc. Am. Bull.*, **111**(2), 275 -290, (1999).
66. D. Smale, J.L. Mauk, J. Palmer, R. Soong, and P. Blattner, Variations in sandstone diagenesis with depth, time, and space, onshore Taranaki wells, New Zealand. *New Zealand Journal of Geology and Geophysics*, **42**, 137-154, (1999).
67. G. Rantitsch, J. Jochum, R.F. Sachsenhofer, B. Russegger, E. Schroll, and B. Horsfield, Hydrocarbon-bearing fluid inclusions in the Drau Range (Eastern Alps, Austria): implications for the genesis of Bleiberg-type Pb-Zn deposits. *Mineral. Petrol.*, **65**(3-4), 141-159, (1999).
68. J. Parnell, P.F. Carey, P. Green, and W. Duncan, Hydrocarbon migration history, west of Shetland; integrated fluid inclusion and fission track studies. *Petroleum Geology of Northwest Europe: Proc. Geol. Soc. London Conf.*, **5**, 613-625, (1999).
69. N.N. Cesaretti, J. Parnell, and E.A. Dominguez, Pore fluid evolution within a hydrocarbon reservoir: Yacoraite formation (upper Cretaceous), northwest basin, Argentina. *J. Pet. Geol.*, **23**(4), 375-398, (2000).
70. J. Lonnee and I.S. Al-Aasm, Dolomitization and fluid evolution in the Middle Devonian Sulphur Point Formation, Rainbow South Field, Alberta: petrographic and geochemical evidence. *Bull. Can. Pet. Geol.*, **48**(3), 262-283, (2000).
71. A.M.E. Marchand, R.S. Haszeldine, C.I. Macaulay, R. Swennen, and A.E. Fallick, Quartz cementation inhibited by cretal oil charge: Miller deep water sandstone, UK North Sea. *Clay Miner.*, **35**(1), 201-210, (2000).
72. R. Thiéry, J. Pironon, F. Walgenwitz, and F. Montel, PIT (Petroleum Inclusion Thermodynamic): a new modeling tool for the characterization of hydrocarbon fluid inclusions from volumetric and microthermometric measurements. *J. Geochem. Explor.*, **69**, 701-704, (2000).
73. J. Parnell, C. Honghan, D. Middleton, T. Haggan, and P. Carey, Significance of fibrous mineral veins in hydrocarbon migration: fluid inclusion studies. *J. Geochem. Explor.*, **69**, 623-627, (2000).
74. D. Middleton, J. Parnell, P. Carey, and G. Xu, Reconstruction of fluid migration history in Northwest Ireland using fluid inclusion studies. *J. Geochem. Explor.*, **69**, 673-677, (2000).
75. D. Lavoie, G. Chi, and M.G. Fowler, The Lower Devonian Upper Gaspé Limestones in eastern Gaspé: carbonate diagenesis and reservoir potential. *Bull. Can. Pet. Geol.*, **49**(2), 346-365, (2001).
76. A. Ceriani, A. Di Giulio, R.H. Goldstein, and C. Rossi, Diagenesis Associated with cooling during burial: An example from Lower Cretaceous Reservoir Sandstones (Sirt Basin, Libya). *AAPG Bull.*, **86**(9), 1573-1591, (2002).
77. C. Rossi, R.H. Goldstein, A. Ceriani, and R. Marfil, Fluid inclusions record thermal and fluid evolution in reservoir sandstones, Khatatba Formation, Western Desert, Egypt: A case for fluid injection. *AAPG Bull.*, **86**(10), 1773-1799, (2002).
78. M. Lisk, G.W. O'Brien, and P.J. Eadington, Quantitative evaluation of the Oil-Leg potential in the Oliver Gas Field, Timor Sea, Australia. *AAPG Bull.*, **86**(9), 1531-1542, (2002).
79. J.L. Mauk and R.C. Burruss, Water Washing of Proterozoic Oil in the Midcontinent Rift System. *AAPG Bull.*, **86**(6), 1113-1127, (2002).
80. H. Volk, B. Horsfield, U. Mann, and V. Suchy, Variability of petroleum inclusions in vein, fossil and vug cements - a geochemical study in the Barrandian Basin (Lower Palaeozoic, Czech Republic). *Org. Geochem.*, **33**(12), 1319-1341, (2002).
81. H.-Y. Tseng and R.J. Pottorf, Fluid inclusion constraints on petroleum PVT and compositional history of the Greater Alwyn-South Brent petroleum system, northern North Sea. *Mar. Pet. Geol.*, **19**(7), 797 809, (2002).
82. A. Dutkiewicz, J. Ridley, and R. Buick, Oil-bearing CO₂-CH₄-H₂O fluid inclusions; oil survival since the Palaeoproterozoic after high temperature entrapment. *Chem. Geol.*, **194**(1-3), 51-79, (2003).
83. A. Dutkiewicz and J. Ridley, Hydrocarbon pseudo-inclusions in barite: How to recognize and avoid artifacts. *J. Sediment. Res.*, **73**(2), 171-176, (2003).

84. A. Dutkiewicz, H. Volk, J. Ridley, and S.C. George, Biomarkers, brines, and oil in the Mesoproterozoic, Roper Superbasin, Australia. *Geology*, **31**(11), 981-984, (2003).
85. M. Feely and J. Parnell, Fluid inclusion studies of well samples from the hydrocarbon prospective Porcupine Basin, offshore Ireland. *J. Geochem. Explor.*, **78-79**, 55-59, (2003).
86. J.R. Boles, P. Eichhubl, G. Garven, and J. Chen, Evolution of a hydrocarbon migration pathway along basin-bounding faults: Evidence from fault cement. *AAPG Bull.*, **88**(7), 947-970, (2004).
87. R. Martinez-Ibarra, J. Tritlla, E. Cedillo-Pardo, J.M. Grajales-Nishimura, and G. Murillo-Muneton, Brine and hydrocarbon evolution during the filling of the Cantarell oil field (Gulf of Mexico). *J. Geochem. Explor.*, **78-79**, 399-403, (2003).
88. A. Dutkiewicz, H. Volk, J. Ridley, and S.C. George, Geochemistry of oil in fluid inclusions in a middle Proterozoic igneous intrusion: implications for the source of hydrocarbons in crystalline rocks. *Org. Geochem.*, **35**(8), 937-957, (2004).
89. R. Jonk, J. Parnell, and A. Whitham, Fluid inclusion evidence for a Cretaceous-Palaeogene petroleum system, Kangerlussuaq Basin, East Greenland. *Mar. Pet. Geol.*, **22**(3), 319-330, (2005).
90. H. Volk, S.C. George, A. Dutkiewicz, and J. Ridley, Characterization of fluid inclusion oil in a mid-Proterozoic sandstone and dolerite (Roper Superbasin, Australia). *Chem. Geol.*, **223**(1-3), 109-135, (2005).
91. A. Dutkiewicz, H. Volk, S.C. George, J. Ridley, and R. Buick, Biomarkers from Huronian oil-bearing fluid inclusions: An uncontaminated record of life before the Great Oxidation Event. *Geology*, **34**(6), 437-440, (2006).
92. C.L. Hanks, T.M. Parris, and W.K. Wallace, Fracture paragenesis and microthermometry in Lisburne Group detachment folds: Implications for the thermal and structural evolution of the northeastern Brooks Range, Alaska. *AAPG Bull.*, **90**(1), 1-20, (2006).
93. M. Brincat, A. Gartrell, M. Lisk, W. Bailey, L. Johnson, and D. Dewhurst, An integrated evaluation of hydrocarbon charge and retention at the Griffin, Chinook, and Scindian oil and gas fields, Barrow Subbasin, North West Shelf, Australia. *AAPG Bull.*, **90**(9), 1359-1380, (2006).
94. C.M. Rott and H. Qing, Analysis of Mississippian anhydrite by fluorescence microscopy - implications for the origin of oil-bearing anhydrite. In *Summary of Investigations 2006, Volume 1, Saskatchewan Geological Survey, Sask, Report 2006-4.1*, 1-11, (2006).
95. R. Wierzbicki, J.J. Dravis, I. Al-Aasm, and N. Harland, Burial dolomitization and dissolution of Upper Jurassic Abenaki platform carbonates, Deep Panuke reservoir, Nova Scotia, Canada. *AAPG Bull.*, **90**(11), 1843-1861, (2006).
96. M. Wilkinson, R.S. Haszeldine, and A.E. Fallick, Hydrocarbon filling and leakage history of a deep geopressured sandstone, Fulmar Formation, United Kingdom North Sea. *AAPG Bull.*, **90**(12), 1945-1961, (2006).
97. M. Baron and J. Parnell, Relationships between stylolites and cementation in sandstone reservoirs: Examples from the North Sea, U.K. and East Greenland. *Sed. Geol.*, **194**(1-2), 17-35, (2007).
98. A. Dutkiewicz, S.C. George, D.J. Mossman, J. Ridley, and H. Volk, Oil and its biomarkers associated with the Palaeoproterozoic Oklo, natural fission reactors, Gabon. *Chem. Geol.*, **244**(1-2), 130-154, (2007).
99. K.E. Higgs, H. Zwingmann, A.G. Reyes, and R.H. Funnell, Diagenesis, porosity evolution, and petroleum emplacement in tight gas reservoirs, Taranaki Basin, New Zealand. *J. Sediment. Res.*, **77**(11-12), 1003-1025, (2007).
100. F. Schubert, L.W. Diamond, and T.M. Toth, Fluid inclusion evidence for petroleum migration through a buried metamorphic dome in the Pannonian Basin, Hungary. *Chem. Geol.*, **244**(3-4), 357-381, (2007).
101. M. Baron, J. Parnell, D. Mark, A. Carr, M. Przyjalowski, and M. Feely, Evolution of hydrocarbon migration style in a fractured reservoir deduced from fluid inclusion data, Clair Field, west of Shetland, UK. *Mar. Pet. Geol.*, **25**(2), 153-172, (2008).
102. J. Bourdet, J. Pironon, G. Levresse, and J. Tritlla, Petroleum type determination through homogenization temperature and vapour volume fraction measurements in fluid inclusions. *Geofluids* **8**(1), 46-59, (2008).
103. R.K. McLimans, Studies of reservoir diagenesis, burial history, and petroleum migration using luminescence microscopy. In Barker, C.E., Kopp, O. (Eds.), *Luminescence Microscopy: Qualitative and quantitative applications*, (SEPM) Short Course 25, 97-106, Society for Sedimentary Geology, Tulsa, USA (1991).
104. R.C. Burruss, K.R. Cercone, and P.M. Harris, Timing of hydrocarbon migration: evidence from fluid inclusions in calcite cements, tectonics and burial history. In: N. Schneidermann, and P.M. Harris (eds.), *Carbonate cements*, Special Publication - Society of Economic Paleontologists and Mineralogists, **36**, 277-289, (1985).

105. N.J.F. Blamey, A.G. Ryder, M. Feely, and P. Owens, Fluorescence lifetime analysis of single hydrocarbon-bearing fluid inclusions – A paragenetic perspective. 23rd IMOG, Torquay, UK, (2007), pp 669-670.
106. S.C. George, M. Ahmed, K. Liu, and H. Volk, The analysis of oil trapped during secondary migration. *Org. Geochem.*, **35**(11-12), 1489-1511, (2004).
107. J. Conliffe, N.J.F. Blamey, M. Feely, J. Parnell, and A.G. Ryder, Hydrocarbon migration in the Porcupine Basin, offshore Ireland: evidence from fluid inclusion studies. *Petroleum Geoscience.*, **16**(1), 67-76, (2010).
108. J.B. Pawley (Ed.). Handbook of Biological Confocal Microscopy, 2nd ed. Plenum Press, New York, (1995).
109. G. Macleod, S.R. Larter, A.C. Aplin, K.S. Pedersen, and T.A. Booth. Determination of the effective composition of single petroleum inclusions using Confocal Scanning Laser Microscopy and PVT simulation. In P.E. Brown, S.G. Hagemann (Eds.), *Biennial Pan-American Conference on Research on Fluid Inclusions (PACROFI VI)* Madison Wisconsin, USA, (1996), pp. 81–82.
110. J. Pironon, M. Canals, M. Dubessy, F. Walgenwitz, and C. Laplace-Builhe, Volumetric reconstruction of individual oil inclusions by confocal scanning laser microscopy. *Eur. J. Mineral.*, **10**(6), 1143-1150, (1998).
111. A.C. Aplin, G. Macleod, S.R. Larter, K.S. Pedersen, H. Sørensen, and T. Booth, Combined use of confocal laser scanning microscopy and PVT simulation for estimating the composition and physical properties of petroleum in fluid inclusions. *Mar. Pet. Geol.*, **16**(2), 97-110, (1999).
112. R. Thiéry, J. Pironon, F. Walgenwitz, and F. Montel, Individual characterization of petroleum fluid inclusions (composition and P-T trapping conditions) by microthermometry and confocal laser scanning microscopy: inferences from applied thermodynamics of oils. *Mar. Pet. Geol.*, **19**(7), 847 -859, (2002).
113. J. Kihle, Adaptation of fluorescence excitation-emission micro-spectroscopy for characterization of single hydrocarbon fluid inclusions. *Org. Geochem.*, **23**(11-12), 1029-1042, (1995).
114. J.A. Musgrave, R.G. Carey, D.R. Janecky, and C.D. Tait, Adaption of Synchronously Scanned Luminescence Spectroscopy to organic-rich fluid inclusion microanalysis. *Rev. Sci. Instrum.*, **65**(6), 1877-1882, (1994).
115. A.C. Aplin, S.R. Larter, M.A. Bigge, G. Macleod, R.E. Swarbrick, and D. Grunberger. Confocal microscopy of fluid inclusions reveals fluid-pressure histories of sediments and an unexpected origin of gas condensate. *Geology*, **28**(11), 1047–1050, (2000).
116. R.E. Swarbrick, M.J. Osborne, D. Grunberger, G.S. Yardley, G. Macleod, A.C. Aplin, S.R. Larter, I. Knight, and H.A. Auld, Integrated study of the Judy Field (Block 30/7a) — an overpressured Central North Sea oil/gas field. *Mar. Pet. Geol.*, **17**(9), 993-1010, (2000).
117. R. Thiéry, J. Pironon, F. Walgenwitz, and F. Montel, Individual characterization of petroleum fluid inclusions (composition and P-T trapping conditions) by microthermometry and confocal laser scanning microscopy: inferences from applied thermodynamics of oils. *Mar. Pet. Geol.*, **19**(7), 847 -859, (2002).
118. P. Stoller, Y. Krüger, J. Rička, and M. Frenz, Femtosecond lasers in fluid inclusion analysis: Three-dimensional imaging and determination of inclusion volume in quartz using second harmonic generation microscopy. *Earth Planet. Sci. Lett.*, **253**(3-4), 359-368, (2007).
119. N.J.F. Blamey, A.G. Ryder, M. Feely, P. Dockery, and P. Owens, The application of structured-light illumination to hydrocarbon-bearing fluid inclusions. *Geofluids*, **8**(2), 102-112, (2008).
120. M.A.A. Neil, R. Juškaitis, and T. Wilson, Method of obtaining optical sectioning by using structured light in a conventional microscope. *Opt. Lett.* **22**(24), 1905-1907, (1997).
121. A.G. Ryder, Quantitative analysis of crude oils by fluorescence lifetime and steady state measurements using 380-nm excitation. *Appl. Spectrosc.*, **56**(1), 107-116, (2002).
122. E.S. Wachman, W.-H. Niu, and D.L. Farkas, AOTF Microscope for imaging with increased speed and spectral versatility. *Biophys. J.*, **73**(3), 1215-1222, (1997).
123. A. Feofanov, S. Sharonov, P. Valisa, E. Dasilva, I. Nabiev, and M. Manfait, A new confocal stigmatic spectrometer for micro-Raman and microfluorescence spectral imaging analysis - design and applications. *Rev. Sci. Instrum.*, **66**(5), 3146 -3158, (1995).
124. E.A.J. Burke, Raman microspectrometry of fluid inclusions. *Lithos*, **55**, 139-158, (2001).
125. J. Jochum, G. Friedrich, D. Leythaeuser, R. Littke, and B. Ropertz, Hydrocarbon-bearing fluid inclusions in calcite-filled horizontal fractures from mature Posidonia Shale (Hils Syncline, NW Germany). *Ore Geol. Rev.*, **9**(5), 363-370, (1995).
126. G. Chi, D. Lavoie, and R. Bertrand, Regional-scale variation of characteristics of hydrocarbon fluid inclusions and thermal conditions along the Paleozoic Laurentian continental margin in eastern Quebec, Canada. *Bull. Can. Petrol. Geol.*, **48**(3), 193-211, (2000).

127. D. Kirkwood, M.M. Savard, and G. Chi, Microstructural analysis and geochemical vein characterization of the Salinic event and Acadian Orogeny: evaluation of the hydrocarbon reservoir potential in eastern Gaspé. *Bull. Can. Petrol. Geol.*, **49**(2), 262-281, (2001).
128. D.W. Morrow, M. Zhao, and L.D. Stasiuk, The gas-bearing Devonian Presqu'île Dolomite of the Cordova embayment region of British Columbia, Canada: Dolomitization and the stratigraphic template. *AAPG Bull.*, **86**(9), 1609-1638, (2002).
129. R. Li and J. Parnell, In situ microanalysis of petroleum fluid inclusions by Time of Flight-Secondary Ion Mass Spectrometry as an indicator of evolving oil chemistry: a pilot study in the Bohai Basin, China. *J. Geochem. Explor.*, **78-9**, 377-384, (2003).
130. D.H.M. Alderton, N.H. Oxtoby, H. Brice, N. Grassineau, and R.E. Bevins, The link between fluids and rank variation in the South Wales Coalfield: evidence from fluid inclusions and stable isotopes. *Geofluids*, **4**(3), 221-236, (2004).
131. I.A. Munz, M. Wangen, J-P. Girard, J-C. Lachapagne, and H. Johansen, Pressure-temperature-time-composition (P-T-t-X) constraints of multiple petroleum charges in the Hild field, Norwegian North Sea. *Mar. Pet. Geol.*, **21**(8), 1043-1060, (2004).
132. D. Lavoie, G. Chi, P. Brennan-Alpert, A. Desrochers, and R. Bertrand, Hydrothermal dolomitization in the Lower Ordovician Romaine Formation of the Anticosti Basin: significance for hydrocarbon exploration. *Bull. Can. Pet. Geol.*, **53**(4), 454-471, (2005).
133. M. Li, L. Stasiuk, R. Maxwell, F. Monnier, and O. Bazhenova, Geochemical and petrological evidence for Tertiary terrestrial and Cretaceous marine potential petroleum source rocks in the western Kamchatka coastal margin, Russia. *Org. Geochem.*, **37**(3), 304-320, (2006).
134. R. Baranger, L. Martinez, J.-L. Pittion, and J. Pouleau, A new calibration procedure for fluorescence measurements of sedimentary organic matter. *Org. Geochem.* **17**(4), 467-475, (1991).
135. U. Resch-Genger, K. Hoffmann, and A. Hoffmann, Standardization of fluorescence measurements - Criteria for the choice of suitable standards and approaches to fit-for-purpose calibration tools. *Annals of the New York Academy of Sciences*, **1130**, 35 -43, (2008)
136. O. Barres, A. Burneau, J. Dubessy, and M. Pagel, Application of Micro-FT-IR Spectroscopy to Individual Hydrocarbon Fluid Inclusion Analysis. *Appl. Spectrosc.*, **41**(6), 1000-1008, (1987).
137. N. Guilhaumou, J.C. Touray, V. Perthuisot, and F. Roure, Palaeocirculation in the basin of southeastern France sub-alpine range: a synthesis from fluid inclusions studies. *Mar. Pet. Geol.*, **13**(6), 695-706, (1996).
138. N. Guilhaumou, N. Ellouz, T.M. Jaswal, and P. Mougín. Genesis and evolution of hydrocarbons entrapped in the fluorite deposit of Koh-i-Maran, (North Kirthar Range, Pakistan). *Mar. Pet. Geol.*, **17**(10), 1151-1164, (2000).
139. Commission Internationale de l'Éclairage (1971) Colorimetry. Publication No. 15. Commission Internationale de l'Éclairage, Paris.
140. Commission Internationale de l'Éclairage (1986) Standard on Colorimetric Observers. CIE S002. Commission Internationale de l'Éclairage, Vienna.
141. Mazères, S., 1997. Mise en oeuvre d'un microspectrofluorimètre pour l'étude de microéchantillons en fluorescence stationnaire et résolue dans le temps. In: Biophysique, Université Paul Sabatier, Toulouse, pp. 200.
142. A. G. Ryder and P. Owens, manuscript in preparation.
143. A.G. Ryder, Assessing the maturity of crude petroleum oils using Total Synchronous Fluorescence Scan Spectra. *J. Fluoresc.*, **14**(1), 99-104, (2004).
144. O. Abbas, C. Rébufa, N. Dupuy, A. Permanyer, J. Kister, and D.A. Azevedo, Application of chemometric methods to synchronous UV fluorescence spectra of petroleum oils. *Fuel*, **85**(17-18), 2653-2661, (2006).
145. G. Ellingsen and S. Fery-Forgues, Application of fluorescence spectroscopy to the study of petroleum: Challenging complexity. *Revue De L Institut Francais Du Petrole*, **53**(2), 201-216, (1998).
146. J.R. Lakowicz, Principles of fluorescence spectroscopy. 3rd Edition, Springer, New York, (2006).
147. A.G. Ryder, Time-resolved fluorescence spectroscopic study of crude petroleum oils: influence of chemical composition. *Appl. Spectrosc.*, **58**(5), 613-623, (2004).
148. A.G. Ryder, T.J. Glynn, and M. Feely. Influence of chemical composition on the fluorescence lifetimes of crude petroleum oils. *Proc SPIE – Int. Soc. Opt. Eng.*, **4876**, 1188-1195, (2003).
149. K. Dowling, M.J. Dayel, S.C.W. Hyde, P.M.W. French, M.J. Lever, J.D. Hares, and A.K.L. Dymoke-Bradshaw. High resolution time-domain fluorescence lifetime imaging for biomedical applications. *J. Mod. Opt.*, **46**(2), 199-209, (1999).
150. M.F. Quinn, A.S. Al-Otaibi, A. Abdullah, P.S. Sethi, F. Al-Bahrani, and O. Alameddine, Determination of intrinsic fluorescence lifetime parameters of crude oils using a laser fluorosensor with a streak camera detection system. *Instrum. Sci. Tech.* **23**(3), 201-215, (1995).

151. A.G. Ryder, T.J. Glynn, M. Przyjalowski, and B. Szczupak. A compact violet diode laser based fluorescence lifetime microscope. *J. Fluoresc.*, **12**(2), 177-180, (2002).
152. P. Owens, A.G. Ryder, and N.J.F. Blamey. Frequency Domain Fluorescence Lifetime Study of Crude Petroleum Oils. *J. Fluoresc.*, **18**(5), 997-1006, (2008).
153. T.W.J. Gadella, T.M. Jovin, and R.M. Clegg, Fluorescence Lifetime Imaging Microscopy (FLIM) - Spatial-Resolution of Microstructures On The Nanosecond Time-Scale. *Biophys. Chem.*, **48**(2), 221-239, (1993).
154. E.B. van Munster, J. Goedhart, G.J. Kremers, E.M.M. Manders, and T.W.J. Gadella Jr., Combination of a spinning disc confocal unit with frequency-domain fluorescence lifetime imaging microscopy. *Cytometry Part A*, **71A**(4), 207-214, (2007).
155. K. Nithipatikom and L.B. McGown, Factors Affecting Calibration for Phase-Modulation Fluorescence Lifetime Determinations. *Appl. Spectrosc.* **40**(4), 549-553, (1986).
156. N.J.F. Blamey, J.F. Conliffe, J.F. Parnell, A.G. Ryder, and M. Feely, Application of fluorescence lifetime measurements on single petroleum-bearing fluid inclusions to demonstrate multi-charge history in petroleum reservoirs. *Geofluids*, **9**, 330-337, (2009).
157. N.J.F. Blamey, A.G. Ryder, P. Owens, and M. Feely. Accurate Characterisation of hydrocarbon-bearing fluid inclusions using frequency domain lifetime measurements. Manuscript in preparation.
158. M.A. Przyjalowski, A.G. Ryder, M. Feely, and T.J. Glynn, Analysis of hydrocarbon-bearing fluid inclusions (HCFI) using time-resolved fluorescence spectroscopy. *Proc. SPIE-Int. Soc. Opt. Eng.*, **5826**, 173-184, (2005).
159. M.A. Przyjalowski, Time-resolved fluorescence spectroscopic analysis of petroleum oils and hydrocarbon bearing fluid inclusions (HCFI), *Ph.D. Thesis*, National University of Ireland, Galway, Galway, Ireland (2006).